UbiQ
targeting the ubiquitin system

UbiQ protocol P008 _ E1 E2 and E3 activity-based probes _ Triple E probes

description: profiling activity of E1, E2 and (HECT/RBR) E3 enzymes with Ub-Dha activity-based probes (Triple E probes).

version: 20220818

reference: Mulder et al. Nature Chemical Biology **2016**, *12*, 523.

General Experimental Conditions E1 labeling assay

1. UBE1 or UBA6 (1 µM) in 50 mM HEPES pH 8, 100 mM NaCl, 10 mM $MgCl_2$ and 250 uM ATP was incubated with probe (30 µM) at 37°C for 30 min.
2. the reaction was quenched by the addition of reducing sample buffer and heating (if required).
3. samples can be analyzed by SDS-PAGE using Coomassie staining.

General Experimental Conditions E2 labeling assay

1. E2 enzyme (2.5 µM) and UBE1 (0.63 µM) in 50 mM HEPES pH 7.5, 100 mM NaCl, 5 mM $MgCl_2$ and 250 uM ATP were incubated with probe (12.5 µM) at 37°C for 30 min.
2. the reaction was quenched by the addition of reducing sample buffer and heating (90°C for 10 min).
3. samples can be analyzed by SDS-PAGE using Coomassie staining.

General Experimental Conditions HECT E3 labeling assay

1. Nedd4L (2.5 µM), UBE2D (0.5 µM) and UBE1 (0.25 µM) were incubated with probe (50 µM) in 50 mM HEPES pH 7.5, 100 mM NaCl, 5 mM $MgCl_2$ and 250 uM ATP at 30°C for 2h.
2. the reaction was quenched by the addition of reducing sample buffer and heating (90°C for 10 min).
3. samples can be analyzed by SDS-PAGE using Coomassie staining.

UbiQ Bio BV
Chamber of Commerce 50023438
VAT NL822502136B01

Science Park **301**
1098 XH Amsterdam
The Netherlands

t +31 20 303 1970
e info@ubiqbio.com
i www.ubiqbio.com

Rabobank
IBAN NL86RABO0150658907
BIC/SWIFT RABONL2U

UbiQ
targeting the ubiquitin system

Proteomic activity profiling of Ub-conjugating enzymes with UbiQ-102.

1. 15-cm dishes of subconfluent HeLa or MelJuSo cells were cultured under standard conditions
2. cells were washed with PBS, trypsinized and centrifuged at 1500 rpm
3. the pellet was washed once with PBS, resuspended in three pellet volumes HR lysis buffer: 50 mM Tris, pH 7.4, 5 mM $MgCl_2$, 250 mM sucrose, 1 mM DTT, and Protease Inhibitor Tablet (Roche)
4. lyse by sonication
5. cell extracts are clarified by centrifugation (20000 rpm, 4 °C, 20 min)
6. total protein concentration was determined using Nanodrop
7. labeling was performed by adding:
   - 10 µg Biotin-Ahx-Ub-Dha (UbiQ-102), 10 mM ATP and 10 mM $MgCl_2$ to 10 mg cell lysates (total protein concentration) in labeling buffer (50 mM HEPES, 100 mM NaCl, 1 mM DTT, pH 8.0)
   - volume is 400 µL, incubate for 1 h at 37 °C while gently shaking.
   - 1 mM ATP and 1 mM $MgCl_2$ were added to the reaction every 15 min. to ensure that the ATP supply is constant
   - for the negative controls: ATP was depleted prior to the reaction using two units of apyrase (Sigma-Aldrich) for 15 min at 37 °C.
   - in case of the negative controls, the labeling reaction was performed as described above, but with the omission of ATP and $MgCl_2$.
8. lysates were incubated for 3 hrs 4 °C with pre-equilibrated High Capacity Neutravidin Agarose (Thermo Fisher) in a total volume of 700 µL while rotating.
9. the supernatant is removed, and the resin washed with 1 mL each of the following wash buffers:
   - 2% SDS in dH_2O)
   - 50 mM HEPES, pH 7.5, 1 mM EDTA, 500 mM NaCl, 1% TritonX-100, 0,1% deoxycholate
   - 10 mM Tris, pH 8.0, 1 mM EDTA, 0,5% NP-40, 250 mM LiCl
   - 50 mM Tris, pH 7.4, 50 mM NaCl.
10. samples are eluted in 40 µL 3× SDS PAGE Loading Buffer (Invitrogen) with additional 2-mercaptoethanol
11. boiled at 95 °C for 5 min
12. before loading onto a 10% gel (NuPAGE, Invitrogen) the proteins were run 1 cm into the gel
13. stain overnight with Coomassie Brilliant Blue
14. destain in dH_2O and cut bands into small pieces using a sterile scalpel
15. process further for LC-MS/MS analysis

UbiQ Bio BV
Chamber of Commerce 50023438
VAT NL822502136B01

Science Park **301**
1098 XH Amsterdam
The Netherlands

t +31 20 303 1970
e info@ubiqbio.com
i www.ubiqbio.com

Rabobank
IBAN NL86RABO0150658907
BIC/SWIFT RABONL2U

ARTICLE
PUBLISHED ONLINE: 16 MAY 2016 | DOI: 10.1038/NCHEMBIO.2084

A cascading activity-based probe sequentially targets E1–E2–E3 ubiquitin enzymes

Monique P C Mulder[1,8], Katharina Witting[1,8], Ilana Berlin[1,8], Jonathan N Pruneda[2], Kuen-Phon Wu[3], Jer-Gung Chang[4], Remco Merkx[1], Johanna Bialas[5], Marcus Groettrup[5], Alfred C O Vertegaal[4], Brenda A Schulman[3,6], David Komander[2], Jacques Neefjes[1], Farid El Oualid[1,7]* & Huib Ovaa[1]*

Post-translational modifications of proteins with ubiquitin (Ub) and ubiquitin-like modifiers (Ubls), orchestrated by a cascade of specialized E1, E2 and E3 enzymes, control a wide range of cellular processes. To monitor catalysis along these complex reaction pathways, we developed a cascading activity-based probe, UbDha. Similarly to the native Ub, upon ATP-dependent activation by the E1, UbDha can travel downstream to the E2 (and subsequently E3) enzymes through sequential trans-thioesterifications. Unlike the native Ub, at each step along the cascade, UbDha has the option to react irreversibly with active site cysteine residues of target enzymes, thus enabling their detection. We show that our cascading probe 'hops' and 'traps' catalytically active Ub-modifying enzymes (but not their substrates) by a mechanism diversifiable to Ubls. Our founder methodology, amenable to structural studies, proteome-wide profiling and monitoring of enzymatic activity in living cells, presents novel and versatile tools to interrogate Ub and Ubl cascades.

Post-translational modifications of cellular targets with Ub or Ubl modules are potent regulators of protein function and thus govern a wide range of biological processes[1]. Although the general biochemical logistics of Ub and Ubl (Ub/Ubl) activation, conjugation and ligation, which are orchestrated sequentially by E1, E2 and E3 enzymes, are highly conserved among eukaryotes, the number and 'flavor' of individual players in each organism's relevant enzymatic repertoire can differ widely[1]. Humans are known to harbor two E1, ~30 E2 and ~600 E3 enzymes in the Ub conjugation cascade, and although some are highly specific for certain targets, others seem to be relatively promiscuous. The complexity of such enzymatic networks, further inundated by ~80 specific proteases responsible for removal of these modifications[1], enables highly specialized and sensitive modes of regulation necessary to accommodate dynamic cellular events. On the flip side, deregulation of these pathways is a common feature in cancer and neurodegenerative and inflammatory diseases. Similarly, some pathogens have evolved to perturb or exploit host Ub/Ubl conjugation cascades to their advantage[2]. The lack of comprehensive tools to assess the enzymology of these processes has posed a longstanding roadblock in the field.

Activity-based probes (ABPs) constitute an important class of reagents used to study enzymatic activity, structure and substrate specificity within the Ub/Ubl modification system[3,4]. In the last decade, researchers have developed various ABPs for deubiquitinating enzymes (DUBs) and Ubl-specific proteases[5–7]. Among the advantages of such probes is their ability to report on DUB activity in cellular extracts and intact cells, thus facilitating study of these enzymes in their biological context[8]. Development of analogous tools for the ligation machinery has proven challenging. Unlike DUBs, which contain highly reactive cysteine nucleophiles, ligases have less nucleophilic active site cysteine residues, rendering them more difficult to trap with electrophiles. Recently, Ubl–AMP probes were reported to selectively label cognate activating enzymes[9–12]. However, because ligation requires transfer of Ub/Ubl between enzymes, the challenge of monitoring reactions throughout the cascade remained. To address this, we developed a mechanism-based ligase probe that undergoes sequential trans-thioesterification reactions as it cascades from the E1 to the E2 and then to the E3 stage. In addition, at each step of the cascade our probe has the option to irreversibly trap the active site cysteine residues of the enzymes in question. This methodology, implemented and characterized with Ub-specific conjugation machinery, is further extended to the NEDD8 enzyme family, demonstrating general applicability of our probe design to Ubls.

The unique properties of our cascading probe enable direct monitoring of sequential E1, E2 and homologous to E6–AP C terminus (HECT)-type E3 activity in a wide variety of experimental settings. Given the ATP dependence of its reactivity against ligases and lack of transfer to substrates, our probe is well suited for proteome-wide profiling of relevant enzymatic cascades. Furthermore, upon introduction into living cells, our probe monitors enzymatic activity of interest and reports on changes in response to chemical or genetic inhibition. From a structural perspective, the probe's stable mechanism-based trapping of catalytic cysteine residues circumvents potential disadvantages incurred by traditional methods of stable E2–Ub conjugate preparation requiring active site mutagenesis[13–17]. Collectively, these features of our ABP tool present previously inaccessible avenues for targeting and monitoring enzymatic activity along the Ub/Ubl conjugation cascades, with implications for drug discovery and for cell and structural biology of these pathways.

RESULTS

Design and synthesis of the cascading ABP

To initiate the Ub/Ubl modification cascade, the E1 activating enzyme adenylates the C terminus of Ub at the expense of ATP, which results in a high-energy E1~Ub thioester formed upon an intramolecular reaction of the intermediate adenylate with the E1 active site cysteine nucleophile. Next, a trans-thioesterification reaction transfers

[1]Division of Cell Biology, Netherlands Cancer Institute, Amsterdam, the Netherlands. [2]Division of Protein and Nucleic Acid Chemistry, Medical Research Council Laboratory of Molecular Biology, Cambridge, UK. [3]Department of Structural Biology, St. Jude Children's Research Hospital, Memphis, Tennessee, USA. [4]Department of Molecular Cell Biology, Leiden University Medical Center, Leiden, the Netherlands. [5]Division of Immunology, Department of Biology, University of Konstanz, Konstanz, Germany. [6]Howard Hughes Medical Institute, Memphis, Tennessee, USA. [7]Present address: UbiQ Bio BV, Amsterdam, the Netherlands. [8]These authors contributed equally to this work. *e-mail: h.ovaa@nki.nl or farideloualid@ubiqbio.com

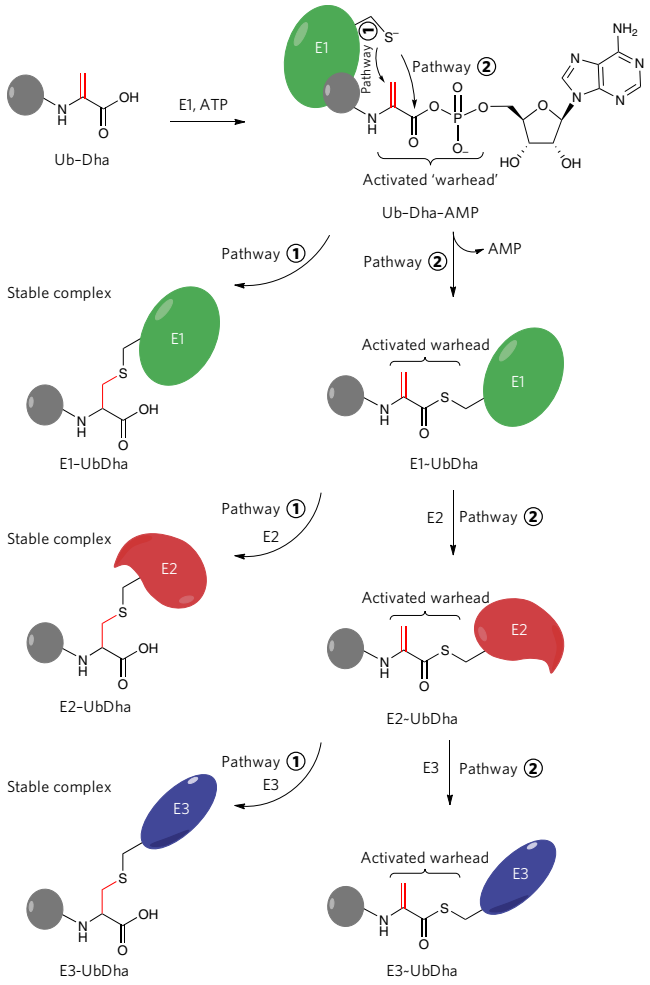

Figure 1 | Mechanism of the ABP UbDha. *In situ* activation of UbDha with E1 and ATP results in a mechanism-based ABP for E1, E2 and cysteine-dependent E3 enzymes. Pathway (**1**) describes the covalent trapping of the enzyme (E–UbDha, thioether-linked adduct), and pathway (**2**) depicts the native trans-thioesterification processing of the probe (E-UbDha, thioester intermediate of conjugate) by the cascade.

the activated Ub to a conserved E2 cysteine, thus forming an E2~Ub thioester intermediate, which subsequently enables transfer of Ub onto a substrate with the help of an E3 (ref. 18). A G76A variant of Ub(Ub-G76A) can also be processed by the E1–E2–E3 cascade but its efficacy is lower[19,20]. We reasoned that replacing the C-terminal alanine by a latent and electrophilic dehydroalanine (Dha) moiety would retain recognition by the E1–E2–E3 enzymes, allowing the Ub-G76Dha (UbDha) to traverse the cascade (**Fig. 1**). Similarly to Ub, UbDha is activated by the E1 enzyme through the formation of an adenylate intermediate, which strongly increases the electrophilic character of the Michael acceptor (Dha moiety). The activated methylene group of the Dha moiety is now poised to either covalently trap the enzyme as an E1–UbDha thioether adduct (**Fig. 1**, pathway (1)) or follow the native ligation route resulting in an E1~UbDha thioester (**Fig. 1**, pathway (2)).

In the second scenario, UbDha is available for transfer to an E2 enzyme, during which the same two events can take place: covalent thioether adduct formation with the probe or a native trans-thioesterification reaction. Lastly, the same is true for the subsequent transfer of UbDha from the E2 to an active site cysteine-dependent E3 (i.e., from the HECT or RING-between-RING (RBR) family of E3 ligases)[21].

UbDha was synthesized starting from Ub(1–75) (**Supplementary Results**, **Supplementary Fig. 1**) using a previously reported linear Fmoc-based solid phase synthesis (SPPS) of Ub[22], where coupling *S*-benzyl-L-cysteine methyl ester (Cys(Bn)-OMe) to the C-terminal carboxyl group of protected Ub(1–75) afforded Ub(1–75)-Cys(Bn)-OMe. After global deprotection with TFA, this was subsequently transformed into UbDha-OMe by oxidative elimination with *O*-mesitylenesulfonylhydroxylamine (MSH)[23]. The methyl ester was then hydrolyzed to generate the UbDha probe. We also used the recently reported 2,5-dibromohexanediamide reagent to convert a cysteine into a Dha moiety[23,24] (**Supplementary Fig. 1**). Notably, in contrast to MSH, 2,5-dibromohexanediamide reacts with a C-terminal cysteine residue and thus allows the use of recombinant Ubl-G76C mutants to prepare probes.

Covalent bond formation with conjugating enzymes

To evaluate the ability of our probe to travel the cascade, we began by subjecting the Ub-activating UBE1 enzyme to UbDha *in vitro*. SDS–PAGE analysis of the reaction revealed formation of an UBE1–UbDha adduct (**Fig. 2a**), consistent with a thioether linkage due to its stability under reducing conditions. ATP dependence of the reaction indicated that the ligation proceeds through the adenylate intermediate (**Fig. 1**). We made similar observations for UBA6 (**Fig. 2a**), the second Ub E1 enzyme to be discovered, which also activates the Ubl modifier FAT10 (ref. 25). To test whether the E1–UbDha thioester can transfer UbDha to the E2 stage, we added UBE2L3 to the reaction. Whereas SDS–PAGE analysis under nonreducing conditions facilitated labeling with both native Ub and UbDha (**Fig. 2b**), only the UbDha probe was able to form a stable adduct with the E2 enzyme under reducing conditions. As expected, we did not observe labeling in the absence of ATP (**Supplementary Fig. 2**). Notably, the double-UbDha-loaded UBE1 intermediate[26] (**Supplementary Figs. 2** and **3**) observed in the absence of an E2 was sensitive to coincubation with UBE2L3 (**Supplementary Fig. 4**), whereas addition of UBE2L3 after UBE1 labeling with UbDha had no effect. This may indicate a transfer of Ub from the adenylation active site to a nearby cysteine in the adenylation domain of UBE1, which does not occur when UbDha is quickly transferred to the next step (here, transfer to E2) in the cascade (ref. 27). In addition to UBE2L3, UbDha showed labeling of 26 other Ub E2s (**Supplementary Fig. 5**) but remained unreactive against Ubl E2s (UBE2F, UBE2I, UBE2L6 and UBE2M). UbDha was also unable to label the Ub E2 UBE2Z downstream of UBE1 owing to the enzyme's selectivity for UBA6 (ref. 25). Noncanonical catalytically inactive E2s UBE2V1 and UBE2V2 (ref. 28) also failed to react with the probe (**Supplementary Fig. 5**). Collectively, these results demonstrate broad utility of the UbDha probe in monitoring mechanism-based transfer of activated Ub from the E1 to a wide range of cognate E2s.

Under nonreducing conditions (**Fig. 2b** and **Supplementary Fig. 6**), a ternary complex of E1~UbDha-E2 was revealed. In this case, the acceptor E2 enzyme reacts directly with the Michael acceptor on the probe-donating E1-thioester adduct. This third pathway of probe action (**Supplementary Fig. 6**) was further confirmed by the stable oxyester linked E1-O~UbDha adduct (**Supplementary Fig. 6**).

Next, we investigated whether UbDha could be further delivered to an E3, bearing an active site cysteine. The family of E3 ligases is subdivided into three major classes according to their mechanism of action[21]. In humans, the known thioester-forming E3s, which harbor catalytic cysteine residues loaded with Ub by a mechanism analogous to the E1 and E2 enzymes, fall into the HECT (28 family members in humans) and RBR (13 members in humans) classes. In contrast, the RING E3 ligases act as scaffolds between the E2~Ub thioester and the substrate protein but do not themselves form thioesters[21]. We therefore examined the well-characterized HECT E3 ligase NEDD4L[14]. As expected, we observed a Cy5–UbDha-NEDD4L thioether adduct downstream of UBE1 and UBE2L3 (**Fig. 2c**). Similarly, a panel of nine other HECT E3s also reacted with the probe (**Supplementary Fig. 7**). Because NEDD4L initially showed

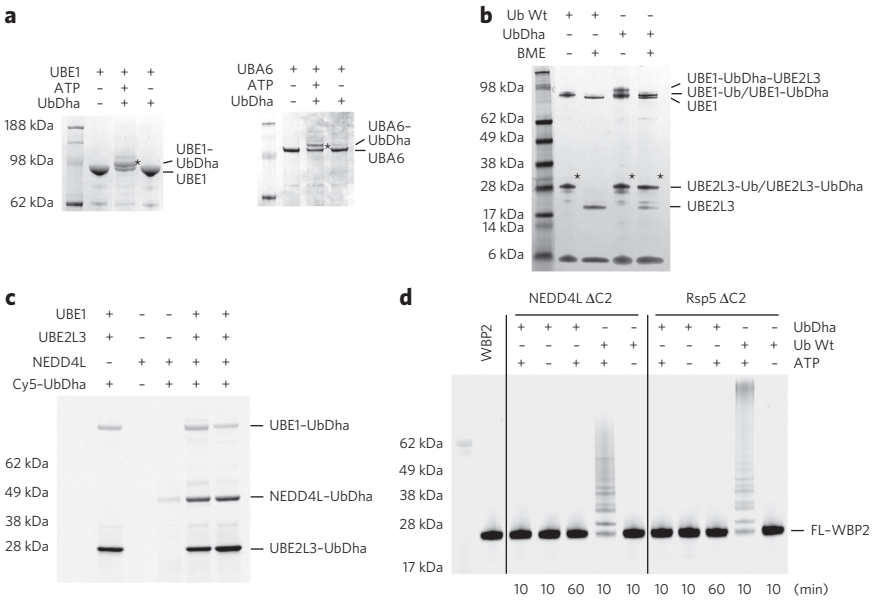

Figure 2 | Covalent thioether bond formation of UbDha with conjugating enzymes. (**a**) ATP-dependent labeling of UBE1 (left) and UBA6 (right). (**b**) Reactivity of UBE2L3 toward Ub and UbDha under reducing and nonreducing conditions. (**c**) Fluorescence scan showing NEDD4L HECT labeling with Cy5–UbDha. (**d**) Multiple-turnover ubiquitination on substrate WBP2 does not occur with UbDha. Asterisks in **a** and **b** indicate modified forms of UBE1, UBA6, UBE2L3 and NEDD4L (full gels are presented in **Supplementary Fig. 19**).

reactivity without ATP (**Supplementary Fig. 7**), we repeated the experiment with an active site Cys-to-Ala mutant and a mutant in which the four noncatalytic cysteine residues were mutated to alanine (4x Cys-to-Ala mutant) (**Supplementary Fig. 8**). Labeling was clearly visible under standard assay conditions, whereas omission of ATP alone or in combination with UBE1 and UBE2D2 resulted in virtually no labeling. Notably, the catalytic Cys-to-Ala mutant showed some labeling albeit less than the wild-type NEDD4L. A similar observation was made for the noncatalytic 4x Cys-to-Ala mutant, suggesting that NEDD4L has at least two cysteines competent to receive an activated UbDha. Not all HECT E3s have a cysteine adjacent to a noncovalent Ub-binding site. For example, the HECT domain of Smurf2 (54% identical to NEDD4L) lacks the candidate cysteine in the noncovalent Ub binding site and showed no alternative labeling of any of its six noncatalytic cysteine residues with our probe (**Supplementary Fig. 9**).

For a native Ub, the next step in the cascade after reactivity with an E3 would result in ligation to a target substrate. To test whether our probe behaves similarly, we chose WBP2 (ref. 29) a known substrate for the UbDha-reactive E3 HECT ligases NEDD4L, Rsp5, WWP1 and WWP2. Although incubation with Ub showed multiple-turnover ubiquitination on WBP2, no ubiquitination was observed with UbDha even with prolonged reaction times (**Fig. 2d** and **Supplementary Fig. 10**). This feature makes UbDha particularly advantageous for enzymatic profiling in cellular systems, where it will remain on the active enzymes irrespectively of the presence of substrates.

Generalizing the cascading ABP methodology to Ubls

To show that our probe design is applicable beyond the Ub cascade, we synthesized an NEDD8-G76C mutant by linear Fmoc-based SPPS[30] and transformed the cysteine into Dha by overnight incubation with 2,5-dibromohexanediamide. After incubation of NEDD8Dha with UBA3–NAE1, SDS–PAGE analysis revealed formation of the expected UBA3–NEDD8 thioether adduct and a double-NEDD8-loaded UBA3 adduct[31] (**Supplementary Figs. 11** and **12**). Coincubation with UBE2M resulted in the formation of a NEDD8–UbE2M thioether adduct (**Supplementary Fig. 11**). As with UBE1, formation of double-NEDD8Dha-linked UBA3 was suppressed when UBE2M was present during E1 labeling. Similarly, treatment with 2-mercaptoethanol had no effect on adduct formation, and labeling with NEDD8Dha failed in the absence of ATP (**Supplementary Fig. 11**). These experiments demonstrate that our cascading ABP design can be extended to other Ubl modification cascades.

E2–Ub thioether adduct structure

To evaluate the structural integrity of our thioether-linked adducts we performed both solution-based and crystallographic studies. Solution properties of the oxyester-linked UBE2N–O~Ub conjugate (in which the active site cysteine has been mutated to serine) have been thoroughly characterized by NMR spectroscopy and small-angle X-ray scattering[32], allowing us to validate the analogous thioether linkage as a suitable mimic. Analysis of chemical shift perturbations in the $^{1}H,^{15}N$ HSQC spectrum of UBE2N (**Supplementary Fig. 13**) arising from conjugation with Ub revealed several regions affected in both the thioether- and oxyester-linked samples (**Fig. 3a**) localized primarily to loop 3, helix 2, loop 8, and the penultimate C-terminal helix (**Fig. 3b**). These perturbed regions can be attributed to the 'closed' conformation of the UBE2N–UbDha thioether adduct, which is predominant in solution[32] and indicates the overall behavior of the thioether-linked adduct to be similar to the oxyester linkage. Certain resonances in the UBE2N–UbDha HSQC spectrum showed markedly different characteristics from that of the oxyester-linked sample (**Fig. 3a**) mapped to the region directly surrounding the active site (**Fig. 3b**). Given the high sensitivity of amide resonances to the local chemical environment, such differences between linkage types are probably due to their differing chemical properties and not to a larger structural change.

Solution studies indicate normal interdomain behavior within the thioether-linked adduct, but they lack the atomic resolution of the linkage and surrounding active site residues. To remedy this, we crystallized the UBE2D3–UbDha adduct under conditions published for the oxyester-linked UBE2D3–O~Ub conjugate[33]. The 2.2-Å UBE2D3–UbDha thioether structure was notably similar to the published oxyester structure (PDB 3UGB), with Cα r.m.s. deviation values of 0.23 and 0.35Å for UBE2D3 and Ub, respectively (**Fig. 3c** and **Supplementary Table 1**). The only substantial deviation between the structures was in the Ub C terminus near the linkage itself, manifested in an r.m.s. deviation of 1.13Å for Ub residues 73–76. The thioether linkage was readily revealed in the corresponding electron density (**Fig. 3d**), although detailed features of the omit map were hampered by high B factors in the flexible Ub C terminus (average B-factor of 105.7 for Ub residues 75–76, compared with 49.4 for all protein). Nearby residues within the UBE2D3 active site were found to adopt nearly identical conformations, with the exception of R90, which was missing from the electron density (**Fig. 3e**). An overlay of the oxyester and thioether structures suggests that the additional carboxylate group of the thioether linkage could displace the arginine side chain from the E2 active site cleft, although to our knowledge there is currently no known role for this residue in E2 catalysis.

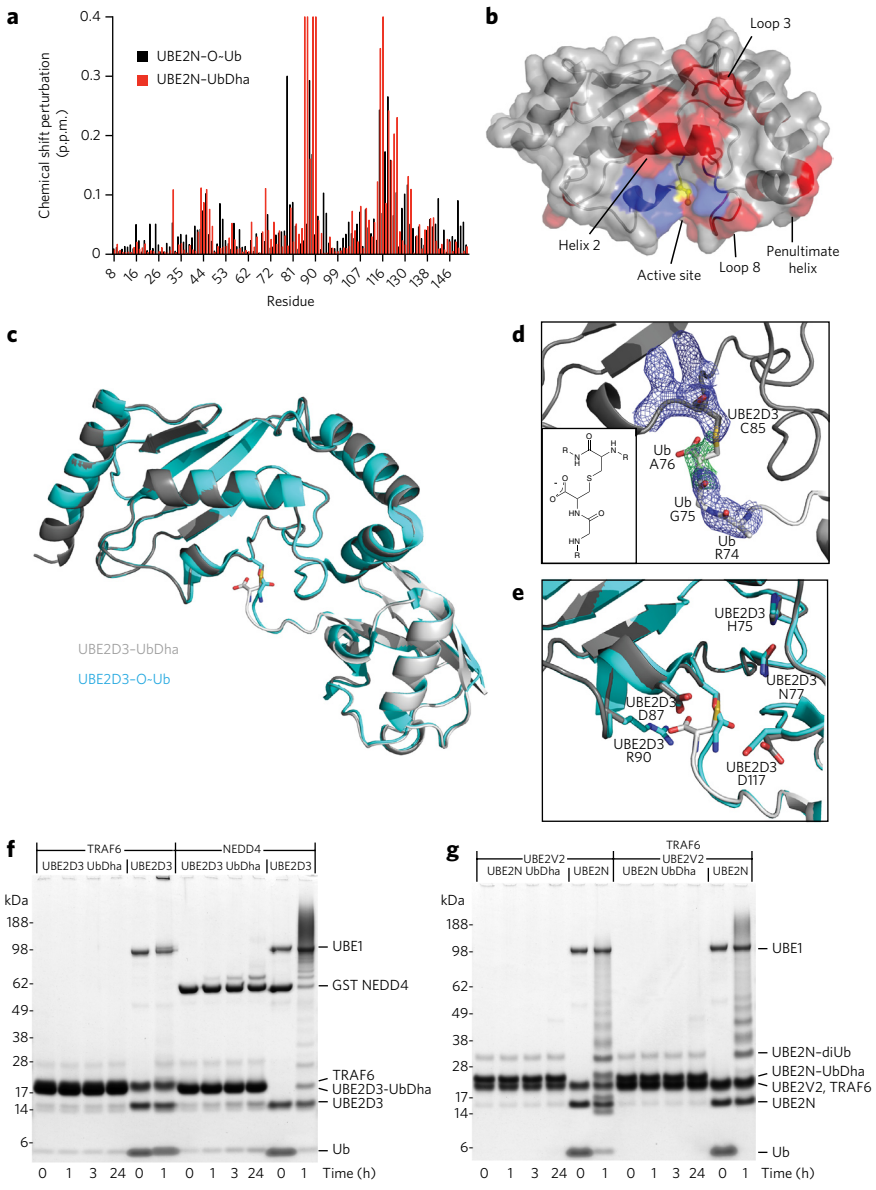

Figure 3 | Structural studies of thioether-linked E2–Ub adducts. (**a**) UBE2N chemical shift perturbations upon Ub activation for oxyester (black) and thioether (red) linkages. Resonances perturbed beyond facile reassignment were plotted using maximum perturbation value. (**b**) Changes from **a** mapped onto the UBE2N structure (PDB 1J7D) (similarities are shown in red; differences in blue). Active site cysteine is shown in yellow. (**c**) Superposition of thioether-linked UBE2D3–UbDha conjugate (gray) over the oxyester-linked form (cyan, PDB 3UGB). (**d**) Simulated annealing omit map of electron density surrounding the thioether linkage. $2|F_o| - |F_c|$ electron density (blue) contoured at 1σ, $|F_o| - |F_c|$ density (green) contoured at 3σ. Inset, structure of the thioether linkage. (**e**) Overlay of E2 active site residues in thioether (gray) and oxyester (cyan) structures. (**f**,**g**) Stability of the thioether-linked UBE2D3- and UBE2N–UbDha adducts, incubated with TRAF6 or NEDD4 (**f**) or UBE2V2 (**g**) alone or in combination with TRAF6.

Preparation of stable E2–Ub conjugates has in the past relied on the dichloroacetone method[13] and oxyester[14–16] and isopeptide[17] bonds, all necessitating mutations to the enzyme's active site. Furthermore, oxyester-linked E2~O–Ub or E2~O–Ubl conjugates are susceptible to hydrolysis, particularly in the presence of an active E3 ligase[14–16], thereby limiting their use in structural applications and preventing any potential utility in cell-based studies. In contrast, UBE2D3–UbDha and UBE2N–UbDha thioether-linked adducts remained inert in the presence of activating factors such as the E3 ligases TRAF6 (RING-type) or NEDD4L (HECT-type) or the accessory E2 variant UBE2V2, with or without TRAF6, respectively (**Fig. 3f**,**g**). As a catalytically inert mimic of native thioester-linked conjugates, the thioether-linked adduct behaved as a competitive inhibitor of the ligation machinery in single-turnover assays monitoring diubiquitin (diUb) formation by UBE2N, UBE2V2 and the E3 ligase cIAP (**Supplementary Fig. 14**). Combined with solution and crystallographic data, these functional assays support the utility of thioether-linked E2–UbDha adducts as stable mimics in both structural and functional studies.

UbDha probe as a proteomics tool

Having validated the activity and structural integrity of the UbDha probe, we turned to enzymatic cascade profiling in biological samples. Incubation of cell extracts with Cy5–UbDha revealed robust labeling of UBE1 (**Fig. 4a**) and UBA6 that was abrogated by apyrase treatment (**Supplementary Fig. 15**). We also detected additional ATP-dependent bands on the same timescale (**Supplementary Fig. 15**), supporting *in vitro* data showing that the probe is passed downstream. To identify these proteins, we used a biotin-labeled probe variant for affinity-based proteomic profiling[3] of human cervical cancer (HeLa) (**Fig. 4b**) and melanoma (MelJuSo) (**Supplementary Fig. 16**) cell extracts. We took advantage of the ATP-dependent reactivity of our probe and conducted affinity-based proteomic profiling in the presence of ATP and with apyrase-mediated ATP depletion. Mass spectrometric analysis of proteins associated with the probe in an ATP-dependent manner retrieved both Ub E1 enzymes and numerous downstream E2 enzymes. Specifically, roughly half of known human E2 enzymes[34] charged by UBE1 (as well as UBE2Z, charged specifically by UBA6) were identified with high confidence in both cell lines. Among the most enriched proteins were UBE2L3, UBE2S and UBE2K, all of which can readily accept Ub from UBE1 and UBA6 (ref. 25). Notably, we recovered three members of the E2D subfamily—UBE2D2, UBE2D3 and UBE2D4—and the largely uncharacterized UBE2D4 was the top hit in HeLa cells (**Fig. 4b**). By contrast, we did not recover UBE2D4 in MelJuSo cells, exemplifying how the UbDha probe can facilitate unbiased proteome-wide comparisons of enzymatic reactivities. In addition to canonical E2s, we detected atypical E2–E3 hybrid enzymes (UBE2O and BIRC6) as well as HECT E3s. Whereas the E3 ligases UBE3A and HECTD1 were found in both cell lines, TRIP12 was observed only in MelJuSo cells. UBE3A prefers to accept Ub from UBE2L3 (ref. 35), which was recovered in high abundance from both cell lines, indicating isolation of a full E1–E2–E3 cascade. Enzymes of interest immunoprecipitated directly from cells can be investigated with the UbDha probe in the presence of supplemented reaction components of choice. This was demonstrated by the ability of GFP–UBE2J1 but not GFP–UBE2Z to accept activated Cy5–UbDha from UBE1 (**Fig. 4c**). As expected, mutation of active site C91 of GFP–UBE2J1 to alanine (C91A) abrogated labeling, demonstrating suitability of UbDha for mutational studies.

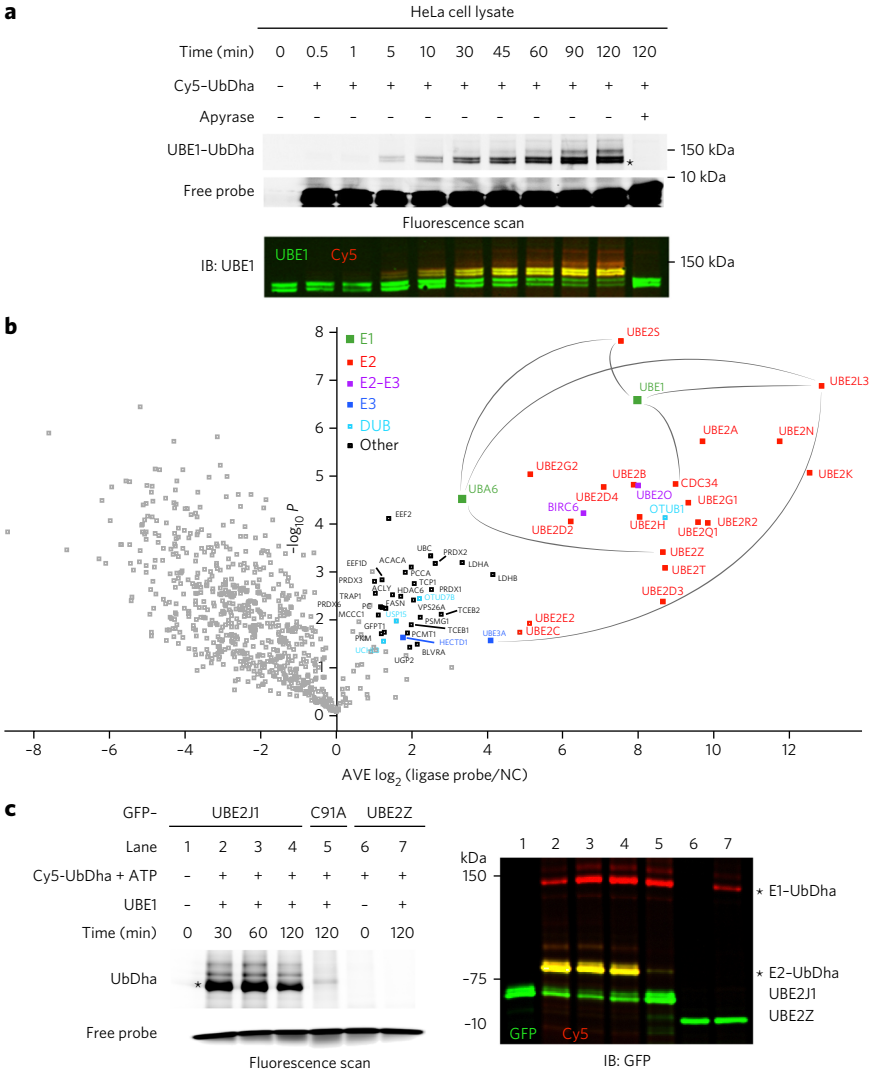

Figure 4 | Proteome-wide activity profiling of Ub-conjugation machinery. (**a**) Time course of UBE1 labeling in HeLa cell extracts with Cy5-UbDha in the absence (−) or presence (+) of ATP scavenger apyrase. IB, immunoblot. (**b**) Proteomic profiling of the Ub activation, conjugation and ligation machineries in HeLa cells. Volcano plot of pairwise comparison of proteins bound to the biotin-UbDha probe relative to apyrase treatment ($-\log_{10} P$ value) as a function of fold enrichment (average $\log_2$) from three technical replicates. Confidently identified proteins (average $\log_2$ ratio >1, $P < 0.05$) are marked as follows: E1, green; E2, red; HECT E3, blue; hybrid E2–E3, purple; DUBs, light blue. Proteins unrelated to the Ub cycle are shown in black, and those falling below the threshold are shown in gray. Gray lines indicate known cascade connections. (**c**) Labeling of GFP-tagged enzymes isolated from HeLa cells (UBE2J1 or its catalytic mutant C91A versus GFP-UBE2Z) with Cy5-UbDha downstream of purified UBE1. A representative experiment is shown ($n = 2$). Asterisks in **a** and **c** indicate modified forms of E1 and E2 enzymes (full-length gels are shown in **Supplementary Fig. 20**).

We also identified four DUBs (OTUB1, OTUD7B, UCHL3 and USP15) in pull-down experiments with the ligase probe (**Fig. 4b** and **Supplementary Fig. 16**). Because DUBs harbor highly reactive active site cysteine residues, we assessed potential cross-reactivity by incubating the Cy5–UbDha probe with cell lysates ectopically expressing various GFP- or FLAG-tagged DUBs (**Supplementary Fig. 17a**) alongside the recently reported DUB-specific ABP, Cy5–UbPA[30]. Whereas Cy5–UbPA readily modified all the active DUBs tested, only incubation with excessive amounts of UbDha resulted in (often marginal) DUB labeling. Moreover, Cy5–UbDha labeling of even highly reactive DUBs such as OTUB1 and OTUB2 was readily abolished by pretreatment with UbPA (**Supplementary Fig. 17b**). Of note, the DUBs recovered with UbDha in our proteomic experiment (particularly OTUB1) can interact with E2 enzymes[36]. As DUB-mediated catalysis proceeds independently of ATP, recovery of these DUBs in the ATP-dependent setting can be a result of isolation together with their active partner ligases.

Activity-based protein profiling in cells

To address the efficacy of UbDha in monitoring the Ub-conjugation cascade in the cellular context, we next introduced Cy5–UbDha into HeLa cells by electroporation. In-gel fluorescence analysis followed by immunoblotting revealed engagement of both UBA6 and UBE1 (**Fig. 5a**) on a timescale similar to or faster than that observed in lysate labeling experiments (**Fig. 4a**). Furthermore, treatment of cells with the UBE1 inhibitor PYR-41 (ref. 37) before introduction of the probe reduced detectable UBE1 activity (**Fig. 5b**), indicating that the probe can be used to monitor enzymatic inhibition in living cells.

Cells harboring Cy5–UbDha showed normal morphology, and the probe was evenly distributed throughout the nuclear and cytoplasmic space, as expected when small molecules such as Ub move unrestricted across the nuclear membrane[38] (**Fig. 5c**, top). Of note, cells undergoing late stages of cell division showed accumulation of Cy5–UbDha at the cytokinetic bridge (**Supplementary Fig. 18**), consistent with the site of BIRC6 activity at this point in the cell cycle[39]. Given that we detected BIRC6 in high abundance in the proteome-wide active ligase analysis (**Fig. 4b**), these observations suggest that our probe could be used to study spatial and/or temporal aspects of relevant enzymatic cascades. For example, introduction of Cy5–UbDha into HeLa cells ectopically expressing predominantly nuclear GFP–UBE1 resulted in the corresponding nuclear accumulation of the probe (**Fig. 5c**,**d**) relative to untransfected cells. In-gel fluorescence analysis and immunoblot analysis of the corresponding lysates confirmed formation of a GFP–UBE1–UbDha adduct (**Fig. 5e**).

To investigate whether the probe can be passed downstream of the E1 while inside the cell, we introduced Cy5–UbDha into cells expressing UBE2J1 or its catalytically inactive C91A or C91S mutants. We observed catalysis-dependent modification of the E2 with the probe (**Fig. 6a**,**b**) that was sensitive to inhibition of the upstream UBE1 (**Fig. 6b**). UBE2J1, which we isolated with UbDha from MelJuSo cell lysates (**Supplementary Fig. 16**), localizes to the endoplasmic reticulum (ER), where it functions in ER-associated degradation (ERAD)[40]. In cells, Cy5–UbDha colocalized with wild-type but not catalytically dead UBE2J1 (**Fig. 6c**,**d**). Notably, this colocalization was sensitive to inhibition of the upstream E1 (**Fig. 6c**,**d**), indicating that imaging of intact cells harboring fluorescently labeled UbDha can report on relevant enzymatic cascades. Collectively, these experiments illustrate a wide range of utilities for UbDha in the study of Ub ligase activity in cells. To our knowledge, UbDha is the first probe that allows cascade-dependent profiling of Ub-conjugating enzymes in a physiologically relevant setting.

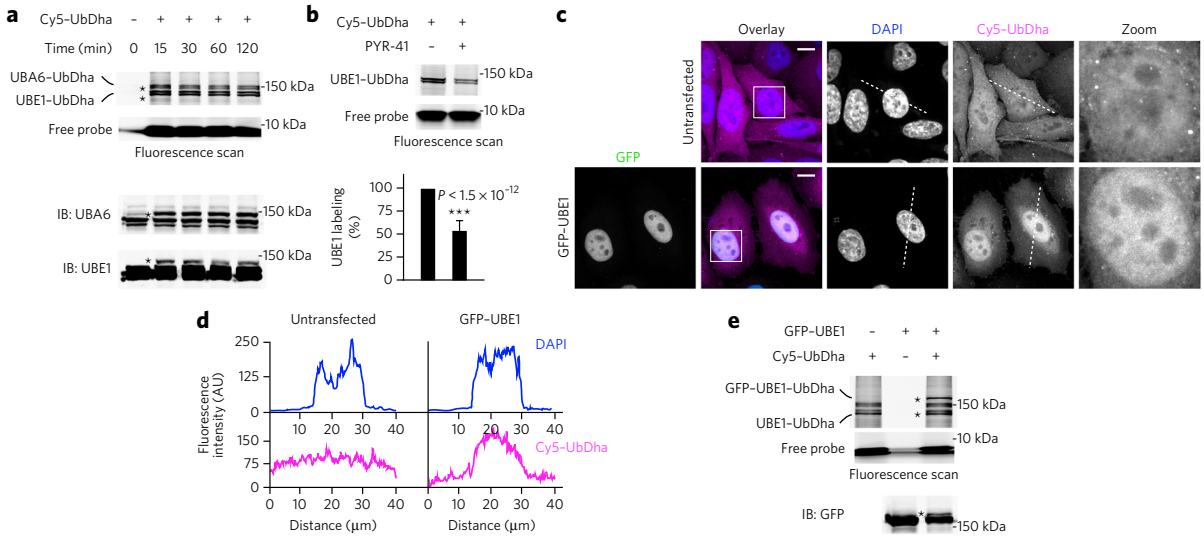

Figure 5 | Activation of UbDha *in vivo*. (**a**) *In vivo* labeling of endogenous E1 enzymes with Cy5–UbDha. Fluorescence scanning and immunoblotting of HeLa cell lysates harvested at indicated time intervals after electroporation of cells with the probe. A representative experiment is shown ($n = 3$). (**b**) Fluorescence scan (top) and quantification (bottom) of *in vivo* labeling of UBE1 with Cy5–UbDha after treatment with PYR-41 (50 μM). Quantification is shown as percentage of labeling in the absence of PYR-41; error bars indicate mean ± s.d. ($n = 3$); significance (P value) was assessed by two-sided t-test. (**c**) Distribution of Cy5–UbDha (magenta) in cells ectopically expressing GFP–UBE1 (green) and in untransfected cells. Representative 3D confocal compilations of fixed cells treated as indicated are shown with DAPI (blue) overlays and nuclear insets ($n = 2$); scale bars, 10 μm. (**d**) Pixel traces of DAPI and Cy5–UbDha (marked with dotted lines in **c**) plotted as fluorescence over distance. AU, arbitrary units. (**e**) Formation of the GFP–UBE1–UbDha adduct in cells. Asterisks in **a** and **e** indicate modified forms of E1 enzymes (full-length gels are shown in **Supplementary Fig. 21**).

DISCUSSION

Given the critical roles of E1, E2 and E3 enzymes in a wide range of biological processes and their resulting emergence as drug targets[41,42], there is a need for suitable assay reagents to study their function. The pyramidal structure of the Ub/Ubl conjugation systems, their complex cross-reactivities and the reactive nature of the E2~Ub and E3~Ub thioester intermediates present practical challenges in dissecting interactions between Ub-loaded partner enzymes. To monitor these enzymatic cascades, we present a unique probe designed to hop from one active site to the next, leaving a detectable covalent mark at each step.

Relatively inert on its own, our cascading probe (UbDha) requires ATP-dependent activation by the E1 enzyme, which increases the electrophilic character of the Dha moiety, making it suitable to follow the cascade of trans-thioesterification reactions downstream. The key conceptual advantage of Dha-based methodology lies in its ability to 'choose' at any point along the cascade between a native-like thioester and irreversible thioether bond formation. We show that UbDha readily labels active site cysteine residues of E1, E2 and HECT E3 enzymes. Notably, UbDha is not transferred to substrates. This feature endows the cascade probe with advantages over the native Ub, particularly in complex biological settings, where enzymes are present together with their substrates. Under such circumstances, UbDha enables direct measure of enzyme activity rather than merely detecting consequences thereof.

Because entry of UbDha (or UblDha) into its cognate enzymatic cascade requires ATP, much of the background binding to the probe can be easily discriminated by eliminating ATP with apyrase. This simple feature makes UbDha suitable for activity-based profiling of Ub/Ubl cascades not only *in vitro* but also in complex biological circumstances, as demonstrated by the proteome-wide analysis of Ub conjugation machineries isolated from two different cancer cell lines. The straightforward nature of the experimental setup is likely to be readily adaptable to comparative profiling of E1, E2 (and some E3 enzymes) as a function

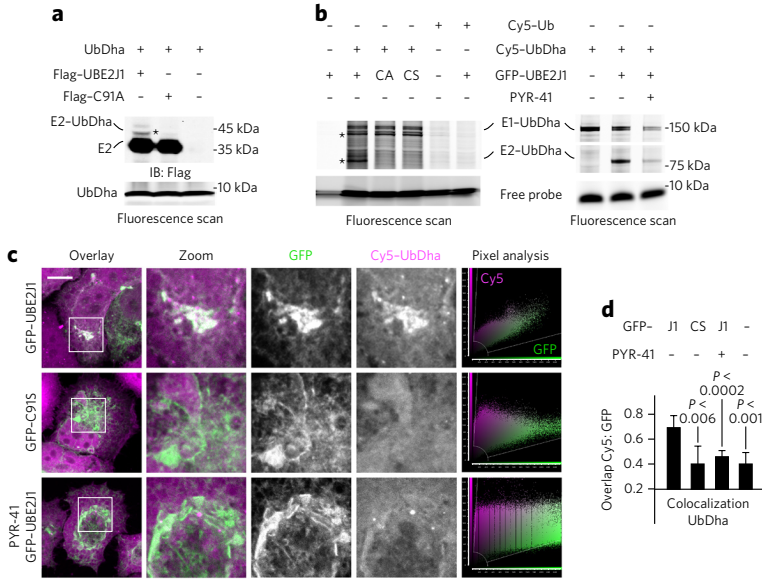

Figure 6 | Probing *in vivo* E1–E2 cascade with UbDha. (**a**) Flag-specific immunoblot (IB) analysis of *in vivo* UbDha adduct formation with Flag-tagged UBE2J1 (Flag–UBE2J1) or its catalytic mutant C91A (Flag–C91A). (**b**) Reactivity of GFP–UBE2J1 and its mutants C91A (CA) or C91S (CS, left) or as a function of UBE1 inhibition (50 μM PYR-41, right) with Cy5–UbDha or Cy5–Ub electroporated into HeLa cells. A representative experiment is shown ($n = 2$). Asterisks in **a** and **b** indicate modified forms of E1 and E2 enzymes. (**c**) Representative 3D confocal compilations of fixed cells (from **b**) treated as indicated. Overlays of GFP (green) with Cy5–UbDha (purple) and corresponding pixel plots are shown ($n = 2$); scale bars, 10 μm. (**d**) Colocalization (Mander's overlap coefficient) of Cy5–UbDha with GFP-tagged wild-type (J1) or mutant (C91S) UBE2J1 ($n = 2$; 10 cells per condition), error bars represent mean ± s.d.; significance (P) assessed by two-sided t-test; full-length gels are shown in **Supplementary Fig. 22**).

of various biological perturbations (such as stimulation, starvation or infection). The same reagent can subsequently be used to study the effects of mutations in enzymes isolated directly from organisms of interest as well as test for relevant factors upstream or downstream in the cascade. At present, standard biochemical techniques for such studies typically involve laborious expression and purification protocols. Furthermore, a lack of observable reactivity in such preparations may be attributable to misfolding or lack of necessary modifications acquired in the carrier organism. Our methodology bypasses these difficulties by offering a relatively quick and easy way to assess reactivity of enzymes isolated directly from cells using simple immunoprecipitation. Then, taking cellular enzymology one step further, UbDha can be introduced into living cells to directly monitor enzymatic activities in their natural context. In this way, the versatility of the UbDha cascade probe may prove invaluable in dissecting how aberrant activities of E1–E2–E3 cascades contribute to pathogenesis[41,42] and for diagnosis and monitoring efficacy of UPS-targeting therapy. Furthermore, by generating a NEDD8-based counterpart of the UbDha probe capable of labeling the NEDD8 conjugating machinery, we show our method to be diversifiable toward Ubls. As such, the technology described here may be used to help interrogate Ubl ligation machineries that are not yet well defined.

In addition to cell-based applications, UbDha (and UblDha) may prove useful *in vitro*, particularly for structure determination. The thioether adducts described here bypass the need for active site mutagenesis[13–17], thus avoiding potential disturbances to catalytic properties of enzymes in question. Stability of our thioether adducts under reducing conditions in the presence of an activating E3 ligase and in functional assays allowed us to perform NMR and X-ray crystallography studies. A high degree of similarity to the published oxyester-linked structure supports their utility as stable mimics in structural and functional studies. We expect that UbDha could be used to expedite generation of crystal structures of E1, E2 or E3 enzymes and their complexes[27]. In addition, we hypothesize that the stability of E2–UbDha adducts immobilized on affinity beads could enable proteomic profiling of cognate RING E3 enzymes, which cannot be directly trapped in a mechanism-dependent manner[43]. On the basis of the proof-of-concept studies described here, we anticipate that our cascading probe reagents will facilitate future discoveries on Ub/Ubl conjugation.

Received 14 January 2016; accepted 22 March 2016; published online 16 May 2016

METHODS

Methods and any associated references are available in the online version of the paper.

Accession codes. The structure of the thioether-linked UBE2D3–UbDha adduct has been deposited under accession code 5IFR.

References

1. Komander, D. & Rape, M. The ubiquitin code. *Annu. Rev. Biochem.* **81**, 203–229 (2012).
2. Steele-Mortimer, O. Exploitation of the ubiquitin system by invading bacteria. *Traffic* **12**, 162–169 (2011).
3. Sadaghiani, A.M., Verhelst, S.H. & Bogyo, M. Tagging and detection strategies for activity-based proteomics. *Curr. Opin. Chem. Biol.* **11**, 20–28 (2007).
4. Cravatt, B.F., Wright, A.T. & Kozarich, J.W. Activity-based protein profiling: from enzyme chemistry to proteomic chemistry. *Annu. Rev. Biochem.* **77**, 383–414 (2008).
5. Borodovsky, A. *et al.* A novel active site-directed probe specific for deubiquitylating enzymes reveals proteasome association of USP14. *EMBO J.* **20**, 5187–5196 (2001).
6. Borodovsky, A. *et al.* Chemistry-based functional proteomics reveals novel members of the deubiquitinating enzyme family. *Chem. Biol.* **9**, 1149–1159 (2002).
7. Ekkebus, R., Flierman, D., Geurink, P.P. & Ovaa, H. Catching a DUB in the act: novel ubiquitin-based active site directed probes. *Curr. Opin. Chem. Biol.* **23**, 63–70 (2014).
8. Kramer, H.B., Nicholson, B., Kessler, B.M. & Altun, M. Detection of ubiquitin-proteasome enzymatic activities in cells: application of activity-based probes to inhibitor development. *Biochim. Biophys. Acta* **1823**, 2029–2037 (2012).
9. Lu, X. *et al.* Designed semisynthetic protein inhibitors of Ub/Ubl E1 activating enzymes. *J. Am. Chem. Soc.* **132**, 1748–1749 (2010).
10. Olsen, S.K., Capili, A.D., Lu, X., Tan, D.S. & Lima, C.D. Active site remodelling accompanies thioester bond formation in the SUMO E1. *Nature* **463**, 906–912 (2010).
11. An, H. & Statsyuk, A.V. Development of activity-based probes for ubiquitin and ubiquitin-like protein signaling pathways. *J. Am. Chem. Soc.* **135**, 16948–16962 (2013).
12. An, H. & Statsyuk, A.V. Facile synthesis of covalent probes to capture enzymatic intermediates during E1 enzyme catalysis. *Chem. Commun. (Camb.)* **52**, 2477–2480 (2016).
13. Wiener, R., Zhang, X., Wang, T. & Wolberger, C. The mechanism of OTUB1-mediated inhibition of ubiquitination. *Nature* **483**, 618–622 (2012).
14. Kamadurai, H.B. *et al.* Insights into ubiquitin transfer cascades from a structure of a UbcH5B approximately ubiquitin-HECT(NEDD4L) complex. *Mol. Cell* **36**, 1095–1102 (2009).
15. Pruneda, J.N. *et al.* Structure of an E3:E2~Ub complex reveals an allosteric mechanism shared among RING/U-box ligases. *Mol. Cell* **47**, 933–942 (2012).
16. Scott, D.C. *et al.* Structure of a RING E3 trapped in action reveals ligation mechanism for the ubiquitin-like protein NEDD8. *Cell* **157**, 1671–1684 (2014).
17. Plechanovová, A., Jaffray, E.G., Tatham, M.H., Naismith, J.H. & Hay, R.T. Structure of a RING E3 ligase and ubiquitin-loaded E2 primed for catalysis. *Nature* **489**, 115–120 (2012).
18. Schulman, B.A. & Harper, J.W. Ubiquitin-like protein activation by E1 enzymes: the apex for downstream signalling pathways. *Nat. Rev. Mol. Cell Biol.* **10**, 319–331 (2009).
19. Hodgins, R.R., Ellison, K.S. & Ellison, M.J. Expression of a ubiquitin derivative that conjugates to protein irreversibly produces phenotypes consistent with a ubiquitin deficiency. *J. Biol. Chem.* **267**, 8807–8812 (1992).
20. Pickart, C.M., Kasperek, E.M., Beal, R. & Kim, A. Substrate properties of site-specific mutant ubiquitin protein (G76A) reveal unexpected mechanistic features of ubiquitin-activating enzyme (E1). *J. Biol. Chem.* **269**, 7115–7123 (1994).
21. Rotin, D. & Kumar, S. Physiological functions of the HECT family of ubiquitin ligases. *Nat. Rev. Mol. Cell Biol.* **10**, 398–409 (2009).
22. El Oualid, F. *et al.* Chemical synthesis of ubiquitin, ubiquitin-based probes, and diubiquitin. *Angew. Chem. Int. Edn Engl.* **49**, 10149–10153 (2010).
23. Bernardes, G.J., Chalker, J.M., Errey, J.C. & Davis, B.G. Facile conversion of cysteine and alkyl cysteines to dehydroalanine on protein surfaces: versatile and switchable access to functionalized proteins. *J. Am. Chem. Soc.* **130**, 5052–5053 (2008).
24. Chalker, J.M. *et al.* Methods for converting cysteine to dehydroalanine. *Chem. Sci. (Camb.)* **2**, 1666–1676 (2011).
25. Jin, J., Li, X., Gygi, S.P. & Harper, J.W. Dual E1 activation systems for ubiquitin differentially regulate E2 enzyme charging. *Nature* **447**, 1135–1138 (2007).
26. Schäfer, A., Kuhn, M. & Schindelin, H. Structure of the ubiquitin-activating enzyme loaded with two ubiquitin molecules. *Acta Crystallogr. D Biol. Crystallogr.* **70**, 1311–1320 (2014).
27. Olsen, S.K. & Lima, C.D. Structure of a ubiquitin E1-E2 complex: insights to E1-E2 thioester transfer. *Mol. Cell* **49**, 884–896 (2013).
28. Andersen, P.L. *et al.* Distinct regulation of Ubc13 functions by the two ubiquitin-conjugating enzyme variants Mms2 and Uev1A. *J. Cell Biol.* **170**, 745–755 (2005).
29. Kee, Y., Lyon, N. & Huibregtse, J.M. The Rsp5 ubiquitin ligase is coupled to and antagonized by the Ubp2 deubiquitinating enzyme. *EMBO J.* **24**, 2414–2424 (2005).
30. Ekkebus, R. *et al.* On terminal alkynes that can react with active-site cysteine nucleophiles in proteases. *J. Am. Chem. Soc.* **135**, 2867–2870 (2013).
31. Walden, H. *et al.* The structure of the APPBP1-UBA3-NEDD8-ATP complex reveals the basis for selective ubiquitin-like protein activation by an E1. *Mol. Cell* **12**, 1427–1437 (2003).
32. Pruneda, J.N., Stoll, K.E., Bolton, L.J., Brzovic, P.S. & Klevit, R.E. Ubiquitin in motion: structural studies of the ubiquitin-conjugating enzyme~ubiquitin conjugate. *Biochemistry* **50**, 1624–1633 (2011).
33. Page, R.C., Pruneda, J.N., Amick, J., Klevit, R.E. & Misra, S. Structural insights into the conformation and oligomerization of E2~ubiquitin conjugates. *Biochemistry* **51**, 4175–4187 (2012).
34. van Wijk, S.J. & Timmers, H.T. The family of ubiquitin-conjugating enzymes (E2s): deciding between life and death of proteins. *FASEB J.* **24**, 981–993 (2010).

35. Huang, L. *et al.* Structure of an E6AP-UbcH7 complex: insights into ubiquitination by the E2-E3 enzyme cascade. *Science* **286**, 1321–1326 (1999).
36. Nakada, S. *et al.* Non-canonical inhibition of DNA damage-dependent ubiquitination by OTUB1. *Nature* **466**, 941–946 (2010).
37. Yang, Y. *et al.* Inhibitors of ubiquitin-activating enzyme (E1), a new class of potential cancer therapeutics. *Cancer Res.* **67**, 9472–9481 (2007).
38. Dantuma, N.P., Groothuis, T.A., Salomons, F.A. & Neefjes, J. A dynamic ubiquitin equilibrium couples proteasomal activity to chromatin remodeling. *J. Cell Biol.* **173**, 19–26 (2006).
39. Pohl, C. & Jentsch, S. Final stages of cytokinesis and midbody ring formation are controlled by BRUCE. *Cell* **132**, 832–845 (2008).
40. Menon, M.B. *et al.* Endoplasmic reticulum-associated ubiquitin-conjugating enzyme Ube2j1 is a novel substrate of MK2 (MAPKAP kinase-2) involved in MK2-mediated TNFα production. *Biochem. J.* **456**, 163–172 (2013).
41. Liu, J. *et al.* Targeting the ubiquitin pathway for cancer treatment. *Biochim. Biophys. Acta* **1855**, 50–60 (2015).
42. da Silva, S.R., Paiva, S.L., Lukkarila, J.L. & Gunning, P.T. Exploring a new frontier in cancer treatment: targeting the ubiquitin and ubiquitin-like activating enzymes. *J. Med. Chem.* **56**, 2165–2177 (2013).
43. Sommer, S., Ritterhoff, T., Melchior, F. & Mootz, H.D. A stable chemical SUMO1-Ubc9 conjugate specifically binds as a thioester mimic to the RanBP2-E3 ligase complex. *ChemBioChem* **16**, 1183–1189 (2015).

Acknowledgments

We thank members of H.O.'s lab for helpful discussion and reagents, J. Brown and S. Armour (Ubiquigent) for providing the E2 scan kit and D. El Atmioui for solid phase peptide synthesis. We acknowledge beamline staff at Diamond I04-1 for expert help. Work was supported by a VICI grant from the Netherlands Organization for Scientific Research (NWO) (724013002) to H.O., a Marie Curie ITN fellowship (290257) to K.W. and EMBO long-term fellowships to I.B. and J.N.P. Work in D.K.'s lab is funded by Medical Research Council (U105192732), the European Research Council (309756), and the Lister Institute for Preventive Medicine. Work in B.A.S.'s lab is funded by ALSAC, HHMI and NIH grant R37GM069530. Work in A.C.O.V.'s lab is funded by the NWO (93511037) and the European Research Council (310913). Work in M.G.'s lab is funded by the German Research Foundation (DFG) CRC969, project C01. J.B. received a stipend from the Graduate School Chemical Biology Ko-RSCB.

Author contributions

M.P.C.M. and F.E.O. designed the study. M.P.C.M., K.W. and I.B. carried out all labeling experiments. I.B. and K.W. designed and executed in-cell labeling experiments with assistance from R.M., and I.B. collected and analyzed confocal microscopy data. Mass spectrometry and relevant data analysis were performed by J.-G.C. and A.C.O.V. on samples prepared by K.W. and I.B. J.N.P. and D.K. performed structural and competition studies and analyzed NMR and X-ray data. K.-P.W. and B.A.S. generated the panel of purified HECT and NEDD8 pathway enzymes and helped with data analysis. J.N. helped with data analysis and provided helpful discussions. J.B. and M.G. provided UBA6. M.P.C.M., F.E.O. and H.O. managed the study. M.P.C.M. and I.B. wrote the manuscript with input from other authors.

Competing financial interests

The authors declare competing financial interests: details are available in the online version of the paper.

Additional information

Any supplementary information, chemical compound information and source data are available in the online version of the paper. Reprints and permissions information is available online at http://www.nature.com/reprints/index.html. Correspondence and requests for materials should be addressed to H.O.

ONLINE METHODS

Chemical synthesis. Detailed procedures for the synthesis of Dha-based ABPs can be found in **Supplementary Note 1**.

Protein expression and purification. The UBE1 enzyme (N-terminal His-tagged) was expressed from a pET3a vector in autoinduction[44] medium at 37 °C using *Escherichia coli* BL21 (DE3). After 2–3 h the temperature was lowered to 18 °C and the bacteria were allowed to grow an additional 12 h. His-tag mediated purification was performed using TALON beads (Clontech) in Buffer A containing 50 mM TRIS (pH 8.0), 150 mM NaCl and 0.25 mM TCEP, washing with 5 mM imidazole (pH 8.0) and eluting with 500 mM imidazole (pH 8.0). Further purification was performed by anion exchange using a Resource Q column (GE Healthcare) and a gradient to 1M NaCl in Buffer A, which was followed by a Superdex 200 column (GE Healthcare).

For the UBE1 C632S mutant, the active site cysteine in UBE1 (C632) was mutated to serine using the protocol provided with the Quik Change Site-Directed Mutagenesis Kit (Invitrogen). The mutant was expressed and purified as described for UBE1.

For His_6–UBA6, a bacmid containing the verified human His_6–UBA6 cDNA sequence was purified from *E. coli* strain DH10Bac using the Quiagen Plasmid Mini Kit (Quiagen) and transfected into SF21 insect cells using the TransIT 2020 transfection reagent (Mirus) leading to the production of baculovirus during three amplification steps according to standard protocols. SF21 cells were infected with the His_6–UBA6 encoding baculovirus and the His_6–UBA6 protein was purified by nickel affinity chromatography using HisTrap matrix (GE Healthcare). The function of the His_6–UBA6 protein was verified by *in vitro* activation assays of recombinant human Ub and the recombinant human Ubl FAT10.

For UBE2N, UBE2V2, and UBE2D3, full-length constructs of UBE2N, UBE2V2, and UBE2D3, and NEDD4 residues 521–900, and cIAP residues 363–614 were expressed from pGEX6P-1 constructs in Rosetta 2 (DE3) pLacI cells (Novagen). TRAF6 residues 50–211 were expressed similarly from the pOPIN-K vector. ^{15}N-labeled UBE2N was expressed in M9 minimal medium supplemented with $[^{15}N]NH_4Cl$. Transformed cells were cultured at 37 °C to an OD_{600} of 0.6–0.8 and induced with 0.2 mM IPTG at 18 °C for 16 h. Cells were lysed by sonication in a buffer containing 25 mM Tris (pH 8.5), 200 mM NaCl, and 4 mM DTT. The clarified lysate was bound to glutathione resin, washed with additional lysis buffer, and the resin was incubated with GST-tagged 3C protease overnight at 4 °C for cleavage of the GST fusion tag, with the exception of NEDD4 and cIAP which were eluted to retain the GST tag. After cleavage, the released protein was washed through the resin, concentrated, and further purified by size-exclusion chromatography on a Superdex 75 column (GE Healthcare) equilibrated in either 20 mM Tris (pH 7.4), 100 mM NaCl, 1 mM DTT for reactions, or 25 mM sodium phosphate (pH 7.0), 150 mM NaCl for NMR spectroscopy. Mouse His–UbE1 was expressed from the pet-24 vector as above and purified by conventional Ni-NTA methods, followed by anion exchange on a Resource Q column and size-exclusion chromatography on a Superdex 200 column (GE Healthcare). Pure fractions of all proteins were concentrated and flash frozen for storage at −80 °C.

For NAE1–UBA3, HECT E3s and WBP2, complexes of GST-tagged NAE1 and UBA3 were coexpressed in *E. coli* RIL strain at 16 °C for 16 h. GST-tagged HECT E3s were expressed in *E. coli* (RIL) at 18 °C overnight. GST-tagged proteins were eluted by 10 mM glutathione followed by proteolysis (thrombin for GST–NAE1, TEV protease for all GST–HECT) at 4 °C overnight and further purified by ionic exchange and size-exclusion chromatography on a Superdex 200 (GE Healthcare) column.

His–MBP-tagged WBP2 was expressed in *E. coli* (RIL) at 20 °C overnight and eluted from Ni-NTA column. TEV protease was applied to remove His–MBP tag. Full-length WBP2 was further purified by ionic exchange using Fast Flow Q column and size-exclusion chromatography on a Superdex 200 column.

Pure proteins were concentrated, aliquoted, flash frozen by liquid nitrogen and stored at −80 °C.

E1–E2–E3 labeling assay conditions. Detailed assay conditions can be found in **Supplementary Note 2**.

Structure determination. *Preparation of thioether-linked [^{15}N]UBE2N–UbDha and UBE2D3–UbDha.* 25 μM UBE1, 250 μM E2 ([^{15}N]UBE2N or UBE2D3), 1 mM UbDha, 5 mM ATP, and 10 mM $MgCl_2$ were incubated at room temperature for 16 h. Any remaining thioester linkages were reduced by the addition of 10 mM DTT at the end of the reaction. The [^{15}N]UBE2N–UbDha adduct was purified to ~95% homogeneity by size-exclusion chromatography on a Superdex 75 column (GE Healthcare) equilibrated in 25 mM sodium phosphate (pH 7.0), 150 mM NaCl. The UBE2D3–UbDha adduct was subsequently purified to >98% homogeneity by repeated cation exchange chromatography on a 6 mL Resource S column (GE Healthcare) with a 50–500 mM NaCl gradient in 50 mM Tris (pH 8.5) buffer, followed by a final size-exclusion chromatography step on a Superdex 75 column (GE Healthcare) equilibrated in 25 mM HEPES, 50 mM NaCl, pH 7.

NMR spectroscopy with [^{15}N]UBE2N–UbDha. ^{1}H,^{15}N BEST-TROSY experiments[45] on 200 μM [^{15}N]UBE2N or [^{15}N]UBE2N–UbDha were acquired with optimized pulse sequences on a Bruker Avance2+ 700MHz spectrometer equipped with a cryogenic triple resonance TCI probe. Data sets were processed using Topspin (Bruker) and visualized with NMRViewJ (One Moon Scientific). Chemical shift perturbations were calculated using the equation $\Delta\delta_j = [(\Delta\delta_j{}^{15}N/5)^2 + (\Delta\delta_j{}^{1}H)^2]^{1/2}$. Perturbation values greater than 0.05 p.p.m. were mapped onto the UBE2N crystal structure (PDB 1J7D), such that the analysis is directly comparable to previous work on the oxyester-linked UBE2N–O~Ub conjugate[32].

Crystallization, data collection and structure determination for UBE2D3–UbDha. The thioether-linked UBE2D3–UbDha adduct was crystallized following conditions published for the oxyester-linked form[33]. Purified conjugate was concentrated to 0.9 mM (23.5 mg/mL) and screened against conditions surrounding the published 200 mM tripotassium citrate, 20% PEG 3350 condition in 200 nL sitting drops at a 1:1 protein/reservoir ratio. The resulting crystals were cryoprotected in LV CryoOil (MiTeGen) and vitrified prior to data collection at Diamond Light Source beamline I04-1. Data were collected at 100K with a wavelength of 0.92 Å. Diffraction images were processed using XDS[46] and scaled using AIMLESS[47]. Isolated UBE2D3 and Ub molecules from the oxyester UBE2D3–O~Ub structure (PDB 3UGB) were used as search models for molecular replacement using PHASER[48]. Iterative model building and refinement were performed using COOT[49] and PHENIX[50], respectively. The thioether linkage could be built unambiguously into the electron density. The final model contained 96.9% in favored, 2.7% in allowed, and 0.4% in outlier Ramachandran space. Data collection and refinement statistics can be found in **Supplementary Table 1**. Structural figures were generated using PyMOL (http://www.pymol.org).

***In vitro* ubiquitination assays.** *Stability.* The stability of thioether-linked UBE2D3–UbDha adduct was assessed by incubating 5 μM purified thioether conjugate at 37 °C in combination with 2 μM TRAF6 or 2 μM GST–NEDD4. The stability of the UBE2N–UbDha adduct was assessed similarlybut with the accessory E2 variant UBE2V2 with or without TRAF6. Samples were collected at 0-, 1-, 3-, and 24-h time points for visualization on Coomassie-stained SDS–PAGE gels. Control reactions containing 0.5 μM UBE1, 5 μM E2, 20 μM Ub and the relevant activating factors demonstrate the Ub chain formation activity under normal *in vitro* conditions.

Competitive inhibition. Single-turnover ubiquitination assays were established for UBE2N with an initial activation stage containing 10 μM UBE2N, 0.5 μM UBE1, 20 μM Ub, 2.5 mM ATP, and 5 mM $MgCl_2$ to generate native thioester-linked UBE2N~Ub after 30 min at 37 °C. This reaction was then quenched by addition of apyrase to prevent any further formation of UBE2N~Ub. Preactivated UBE2N~Ub was then diluted twofold into a reaction containing 5 μM UBE2V2 alone or in addition to 1 μM GST–cIAP, and samples were collected at 0-, 15-, and 30-min time points for visualization of diUb product formation on Coomassie-stained SDS–PAGE gels. To test for competitive inhibition using the thioether-linked UBE2N–UbDha adduct, increasing concentrations (1.25 μM, 2.5 μM, 5 μM, 10 μM, and 20 μM) of purified conjugate were added to reactions containing UBE2N~Ub, UBE2V2, and GST–cIAP as specified above, and samples were collected at 30-min intervals to compare levels of diUb product formation with the control experiment.

Mammalian cell lines. HEK293T and HeLa cell lines used in this study originated from ATCC and were cultured under standard conditions in DMEM (Gibco) supplemented with 10% FCS (Sigma-Aldrich) at 37 °C with 5% CO_2. The previously characterized human melanoma cell line MelJuSo[51] was cultured in IMDM (Gibco) supplemented with FCS. All cell lines were routinely tested for mycoplasma contamination with consistently negative outcome.

Labeling of overexpressed DUBs in cell lysates. For overexpression of epitope-tagged DUBs in HEK293T cells, previously described wild-type and catalytic point mutants of USP8, OTUB1 and OTUB2 were used[30]. Additionally, human USP15 and OTUD1 were subcloned from pDEST-cDNA constructs (Addgene) into 2xFLAG-C1 vector (Clontech) at HindIII and XbaI or XhoI and EcoRI sites, respectively, and mutagenesis of catalytic residues C269S in USP15 and C320S in OTUD1 was performed using standard protocols (Stratagene). DNA was delivered into HEK293T cells using polyethylenimine (PEI, Polysciences, Inc.) according to the manufacturer's instructions. 24h after transfection, cells were harvested by scraping in lysis buffer (150 mM NaCl, 50 mM Tris-HCl, pH 7.5, 0.5% TritonX-100, Protease Inhibitor tablet (Roche)), and lysate was clarified by centrifugation. Reactions were incubated in the presence of indicated components with either Cy5–UbPA (1.0 µg/reaction, stationary for 30–45 min at room temperature (RT)) or Cy5–UbDha (1.5 µg/reaction with gentle agitation for 70 min at 37 °C) in the presence of 10 mM ATP and 10 mM $MgCl_2$. 10 mM NMM was added where indicated. Preincubation with unlabeled UbPA (1.5 µg/reaction) was performed as for Cy5–UbPA followed by Cy5-UbDha chase as above. Reactions were stopped by the addition of sample loading buffer supplemented with 100 mM DTT and boiled for 10 min. Samples were resolved using standard SDS–PAGE, and probe reactivity was assessed by Cy5 fluorescence scanning (λ excitation = 625 nm; λ emission = 680 nm), followed by gel transfer onto nitrocellulose membranes and immunoblotting with either rabbit anti-GFP serum[52], mouse anti-Flag (1:1,000 dilution; Sigma-Aldrich, Sigma F3165) or mouse anti-β-actin (1:10,000 dilution; Sigma-Aldrich A544), as indicated. Fluorescent secondary antibodies anti-mouse-800 (1: 10,000 dilution; LiCOR, 926-3210) and anti-rabbit-800 (1: 10,000 dilution; LiCOR, 926-3211) were used for visualization of labeled proteins on LICOR Odyssey system v3.0.

Cell lysate labeling. Cell lysates were prepared by resuspending cell pellets in three pellet volumes of HR buffer (50 mM TRIS, pH 7.4, 5 mM $MgCl_2$, 250 mM sucrose, 1 mM DTT) and lysed by sonication. After clarification by centrifugation (20,000 r.p.m., 4 °C, 20 min), total protein concentration was determined by Nanodrop. For the labeling experiments, 100 µg lysate was incubated with 0.5 µg Cy5–UbDha, 10 mM ATP and 10 mM $MgCl_2$ in labeling buffer (50 mM HEPES, 100 mM NaCl, pH 7.5) at 37 °C for 1h or as indicated. Additional 1 mM ATP and $MgCl_2$ were added to the reaction every 20 min to replenish consumed ATP. In case of the negative control, lysates were treated with 2 units apyrase (Sigma-Aldrich) prior to addition of the Cy5–UbDha probe (ATP and $MgCl_2$ were omitted). The reaction was terminated by the addition of 3×SDS–PAGE Loading Buffer (Invitrogen) containing β-mercaptoethanol. Samples were resolved by SDS–PAGE and visualized by fluorescence scanning (λ excitation = 625 nm; λ emission = 680 nm). For visualizing the reactivity of endogenous UBE1 and UBA6, immunoblotting was performed as previously described, and membranes were probed with rabbit anti–UbE1 (1:1,000 dilution; Abcam 181225) or rabbit anti-UBA6 (1:1,000 dilution; Abcam 177514).

Activity-based Ub cascade profiling in intact cells. *Electroporation of UbDha into living cells*. HeLa cells cultured under standard growth conditions were transfected with GFP, GFP–UBE1 (ref. 53), GFP–UBE2J1, GFP-tagged UBE2J1 or mutants C91A or C91S, and Flag-tagged UBE2J1 or mutant C91A using Effectene (Qiagen), according to the manufacturer's instructions. To facilitate the incorporation of the probe, the growth medium was refreshed 4–6 hafter transfection and again 1–2 hbefore electroporation. For inhibition of UBE1, cells were treated with 50 µM PYR-41 for 30 min prior to introducing the probe. Following removal of the growth medium, cells were kept on ice for the duration of the protocol. Cells were washed twice with cold electroporation buffer (2 mM HEPES, pH 7.4, 15 mM $K_2HPO_4/KHPO_4$, 250 mM mannitol, 1 mM $MgCl_2$). 1.5 mL of a solution of the Cy5–UbDha, Cy5–Ub or rhodamine–UbDha probe in electroporation buffer (0.4 mg/mL) was added to each of the wells and electroporation was performed on ice using a Biorad GenePulser Xcell with CE and PE module Pulse Generator equipped with a Petri Pulser electroporation applicator (BTX) using the following settings: square wave, voltage=75 V, pulse length=3 ms, pulse interval=1.5 s, number of pulses=5, cuvette width=2 mm. The electroporation applicator was turned 90 degrees, and electroporation was repeated once. The probe solution was replaced by cold electroporation buffer, and cells were allowed to recover on ice for 2 min. After treatment, cells were washed twice with ice-cold PBS and allowed to recover under standard growth conditions as indicated (15–120 min).

For gel-based analysis, samples were lysed using reducing SDS–PAGE loading buffer followed by brief sonication and heating at 98 °C for 10 min before being analyzed on SDS–PAGE gel, and subsequently visualized by fluorescence scanning scanning (λ_{ex} = 625 nm; λ_{em} = 680 nm (Cy5–UbDha) or λ_{ex} = 473 nm; λ_{em} = 530 nm (Rho–UbDha)). Western blotting was performed as described above, and membranes were probed with rabbit anti-GFP serum[52] or mouse anti-Flag (1:1,000 dilution; Sigma-Aldrich, Sigma F3165).

Confocal microscopy. For microscopy experiments, the samples were fixed in 4% formaldehyde (Merck) in PBS and mounted onto glass slides (Thermo Scientific) using Prolong Gold mounting medium with DAPI (Invitrogen). *Z* stacks of 5 images per cell were collected on a Leica SP5 confocal microscope equipped with HyD detectors, using a 63× magnification lens in combination with 2.5–4× digital zoom and represented as maximum *z* projections. Image processing and fluorescence intensity analysis were performed using ImageJ64 software, and colocalization was expressed in the form of Mander's overlap coefficients calculated using JACoP. Pixel plot analyses were generated using Leica LASAF software.

Statistics and reproducibility. Statistical data are presented as mean ± standard deviation (s.d.). Comparisons between the samples were made using a two-sided *t*-test (assessed against controls). Data analyzed were derived from at least two biologically independent experiments (*n*) as indicated in figure legends.

Proteomic activity profiling of Ub-conjugating enzymes. *Sample preparation*. For identification of enzymes reactive towards the biotin–UbDha probe, 15-cm dishes of subconfluent HeLa or MelJuSo cells were cultured under standard conditions. Cells were washed with PBS, trypsinized and centrifuged at 1,500 r.p.m. The pellet was washed once with PBS, resuspended in three pellet volumes HR lysis buffer (50 mM Tris, pH 7.4, 5 mM $MgCl_2$, 250 mM sucrose, 1 mM DTT, and Protease Inhibitor Tablet (Roche)) and lysed by sonication. After sonication, the cell extracts were clarified by centrifugation (20,000 r.p.m., 4 °C, 20 min), and the total protein concentration was determined using Nanodrop. Labeling was performed by adding 10 µg biotin–UbDha, 10 mM ATP, 10 mM $MgCl_2$ to 10 mg cell lysates (total protein concentration) in labeling buffer (50 mM HEPES, 100 mM NaCl, 1 mM DTT, pH 8.0) in a volume of 400 µL for 1 h at 37 °C while gently shaking. To ensure that the ATP supply is constant, 1 mM ATP and 1 mM $MgCl_2$ were added to the reaction every 15 min. For the negative controls, ATP was depleted prior to the reaction using two units of apyrase (Sigma-Aldrich) for 15 min at 37 °C. In case of the negative controls, the labeling reaction was performed as described above, but with the omission of ATP and $MgCl_2$. After reaction with the probe, the lysates were incubated with pre-equilbrated High Capacity Neutravidin Agarose (Thermo Fisher) for 3 h at 4 °C in a total volume of 700 µL while rotating. Subsequently, the supernatant was removed and the resin was washed with 1 mL each of the following wash buffers[54]: buffer 1 (2% SDS in dH_2O), buffer 2 (50 mM HEPES, pH 7.5, 1 mM EDTA, 500 mM NaCl, 1% TritonX-100, 0,1% deoxycholate), buffer 3 (10 mM Tris, pH 8.0, 1 mM EDTA, 0,5% NP-40, 250 mM LiCl) and buffer 4 (50 mM Tris, pH 7.4, 50 mM NaCl). After washing, the samples were eluted in 40 µL 3× SDS PAGE Loading Buffer (Invitrogen) with additional 2-mercaptoethanol and boiled at 95 °C for 5 min before loading onto a 10% gel (NuPAGE, Invitrogen). The proteins were run 1 cm into the gel and subsequently stained overnight with Coomassie Brilliant Blue before being destained in H_2O. After destaining, the band was cut into small pieces using a sterile scapel and processed further for LC-MS/MS analysis.

LC-MS/MS analysis. In-gel digested peptides were cleaned and desalted by 1 ml 0.1% formic acid twice on OASIS HLB cartridge (Waters) before being eluted twice with 100 µL 80% acetonitrile in 0.1% formic acid. Desalted peptides

doi:10.1038/nchembio.2084

were vacuum centrifuged at room temperature until complete dryness then dissolved in 0.1% formic acid prior to online nanoflow LC-MS/MS. The analysis of in-solution-digested peptides was performed using an EASY-nLC system (Proxeon) connected to a QExactive (Thermo Scientific) using higher-collisional dissociation (HCD) fragmentation. Separation of peptides was performed using 13-cm long analytical columns (ID 75 µm, Polymicro Avantes) packed inhouse with 1.8 µm C18 beads (Reprospher-DE, Pur, Dr. Maisch), using a 30-min gradient from 2% to 95% acetonitrile in 0.1% formic acid and a flow rate of 200 nL per minute. The mass spectrometer was operated in data-dependent acquisition mode using a top 10 method. Full-scan MS spectra were acquired with a target value of 3E6 and a resolution of 70,000, with a scan range from 400 to 1,400 *m*/*z*. HCD MS/MS spectra were acquired using a target value of 1E5, a resolution of 17,500, and a normalized collision energy of 25%. All charges lower than two and higher than six were rejected, and all unknown charges were rejected. The underfill ratio was set to 1.0%, and a dynamic exclusion of 60 s was used.

Data processing. MaxQuant version 1.5.1.2 was used to analyze all RAW data[55,56]. The experiment was performed with biological triplicates and measured as three technical replicates. MS/MS spectra were filtered and deisotoped, and the 18 most abundant fragments for each 100 *m*/*z* were retained. MS/MS spectra were filtered for a mass tolerance of 6 p.p.m. for precursor masses, and a mass tolerance of 20 p.p.m. was used for fragment ions. Peptide and protein identification was performed through matching the identified MS/MS spectra versus a target-decoy version of the complete human UniProt database (as of 3 December 2015, 92,040 proteins), in addition to a database of 245 commonly observed MS contaminants. Up to two missed tryptic cleavages were allowed. Cysteine carbamidomethylation was set as a fixed peptide modification. Protein N-terminal acetylation and methionine oxidation were set as variable peptide modifications. Peptides were accepted with a minimum length of six amino acids, a maximum size of 6 kDa, and a maximum charge of six. The processed data were filtered by posterior error probability (PEP) to achieve a protein false discovery rate (FDR) <1%, a peptide-spectrum match FDR <1%. Modified peptides were additionally filtered to have an Andromeda score of at least 40.

Label-free quantification (LFQ). Label-free quantification was performed using MaxQuant LFQ. Quantification was performed over three biological replicates. The fast LFQ algorithm was used with default settings (minimum ratio count of two, minimum neighbors of three, average neighbors of six). Protein LFQ values were $\log_2$transformed for further processing. Proteins identified by site only, reverse sequence only and potential contaminants were removed. Proteins identified by at least fourMS/MS spectra, at least tworazor+unique peptides and at least one unique peptide were retained. To ensure biological reproducibility, only proteins detected in at least two out of the three biological replicates in at least one group were retained. Subsequently, missing values were imputed using Perseus software version 1.5.1.6 with standard settings. LFQ values were averaged within all treatment conditions. Proteins were considered to have a specific interaction with the Ub ligase probe when they were enriched at least twofold compared to the negative control with a *t*-test *P* value <0.05.

44. Studier, F.W. Protein production by auto-induction in high density shaking cultures. *Protein Expr. Purif.* **41**, 207–234 (2005).
45. Favier, A. & Brutscher, B. Recovering lost magnetization: polarization enhancement in biomolecular NMR. *J. Biomol. NMR* **49**, 9–15 (2011).
46. Kabsch, W. Xds. *Acta Crystallogr. D Biol. Crystallogr.* **66**, 125–132 (2010).
47. Winn, M.D. *et al.* Overview of the CCP4 suite and current developments. *Acta Crystallogr. D Biol. Crystallogr.* **67**, 235–242 (2011).
48. McCoy, A.J. *et al.* Phaser crystallographic software. *J. Appl. Crystallogr.* **40**, 658–674 (2007).
49. Emsley, P., Lohkamp, B., Scott, W.G. & Cowtan, K. Features and development of Coot. *Acta Crystallogr. D Biol. Crystallogr.* **66**, 486–501 (2010).
50. Adams, P.D. *et al.* The Phenix software for automated determination of macromolecular structures. *Methods* **55**, 94–106 (2011).
51. Johnson, J.P., Demmer-Dieckmann, M., Meo, T., Hadam, M.R. & Riethmüller, G. Surface antigens of human melanoma cells defined by monoclonal antibodies. I. Biochemical characterization of two antigens found on cell lines and fresh tumors of diverse tissue origin. *Eur. J. Immunol.* **11**, 825–831 (1981).
52. van der Kant, R. *et al.* Late endosomal transport and tethering are coupled processes controlled by RILP and the cholesterol sensor ORP1L. *J. Cell Sci.* **126**, 3462–3474 (2013).
53. Sugaya, K., Ishihara, Y., Inoue, S. & Tsuji, H. Characterization of ubiquitin-activating enzyme Uba1 in the nucleus by its mammalian temperature-sensitive mutant. *PLoS One* **9**, e96666 (2014).
54. Roux, K.J., Kim, D.I., Raida, M. & Burke, B. A promiscuous biotin ligase fusion protein identifies proximal and interacting proteins in mammalian cells. *J. Cell Biol.* **196**, 801–810 (2012).
55. Cox, J. *et al.* Andromeda: a peptide search engine integrated into the MaxQuant environment. *J. Proteome Res.* **10**, 1794–1805 (2011).
56. Cox, J. & Mann, M. MaxQuant enables high peptide identification rates, individualized p.p.b.-range mass accuracies and proteome-wide protein quantification. *Nat. Biotechnol.* **26**, 1367–1372 (2008).

Supplementary Information

A cascading activity-based probe sequentially targets E1-E2-E3 ubiquitin enzymes

Monique P.C. Mulder[1,*], Katharina Witting[1,*], Ilana Berlin[1,*], Jonathan N. Pruneda[2], Kuen-Phon Wu[3], Jer-Gung Chang[4], Remco Merkx[1], Johanna Bialas[6], Marcus Groettrup[6], Alfred C.O. Vertegaal[4], Brenda A. Schulman[3,5], David Komander[2], Jacques Neefjes[1], Farid El Oualid[1,7,§], Huib Ovaa[1,§]

1) Division of Cell Biology, Netherlands Cancer Institute, Plesmanlaan 121, 1066 CX Amsterdam, The Netherlands
2) Division of Protein and Nucleic Acid Chemistry, Medical Research Council Laboratory of Molecular Biology, Francis Crick Avenue, Cambridge, CB2 0QH, United Kingdom
3) Department of Structural Biology, St. Jude Children's Research Hospital, 262 Danny Thomas Place, Memphis, TN 38105, USA.
4) Department of Molecular Cell Biology, Leiden University Medical Center, Albinusdreef 2, 2333 ZA Leiden, the Netherlands
5) Howard Hughes Medical Institute, 262 Danny Thomas Place, Memphis, TN 38105, USA.
6) Division of Immunology, Department of Biology, University of Konstanz, D-78457 Konstanz, Germany
7) Current address: UbiQ Bio BV, Science Park 408, 1098 XH, Amsterdam, The Netherlands

*) Co-first author

[§]) To whom correspondence should be addressed: h.ovaa@nki.nl or farideloualid@ubiqbio.com.

Nature Chemical Biology: doi:10.1038/nchembio.2084

Supplementary Results

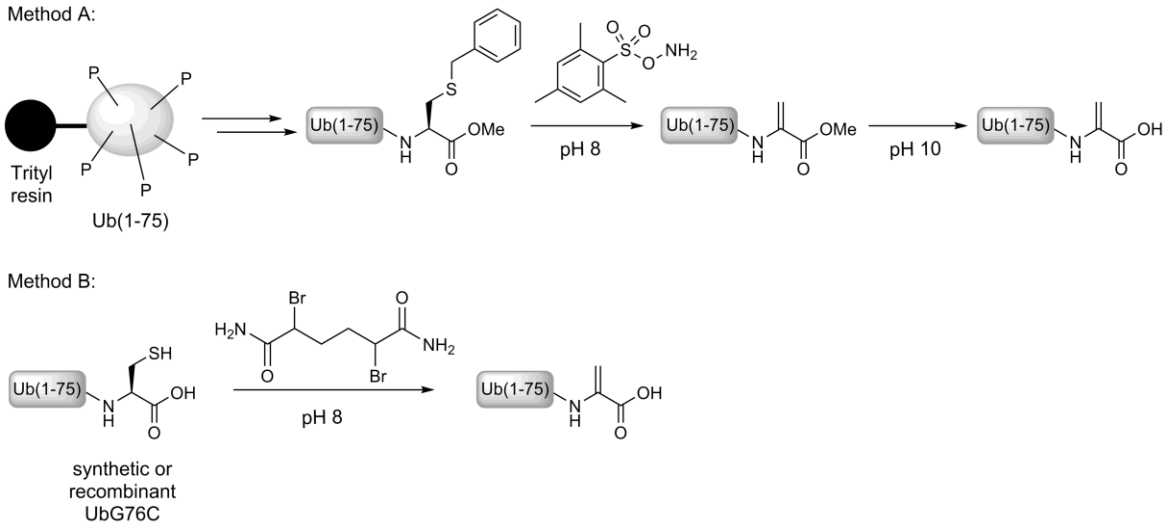

Supplementary Figure 1. Synthesis of Ub-Dha starting from Ub(1-75)-Cys(Bn)-OMe (method A) or UbG76C (method B).

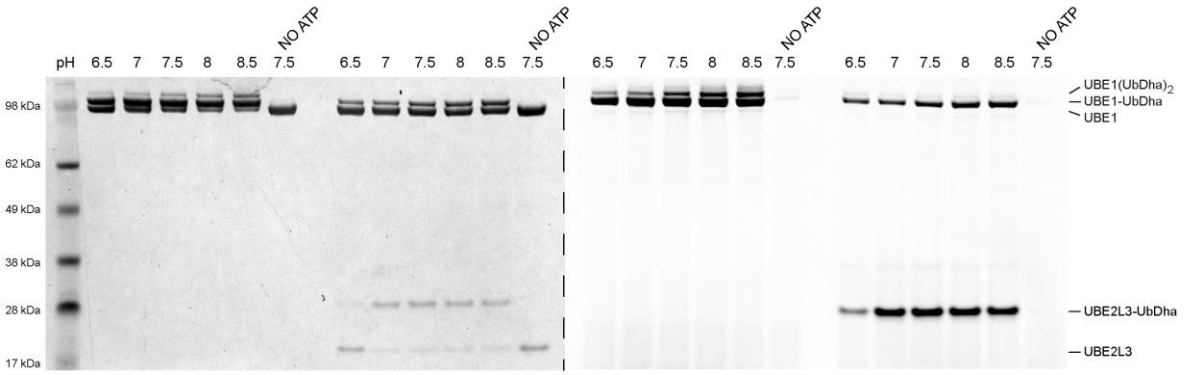

Supplementary Figure 2. pH effect on labeling of Cy5-UbDha with UBE1 and UBE2L3. Left: silver stain, right: fluorescent scan.

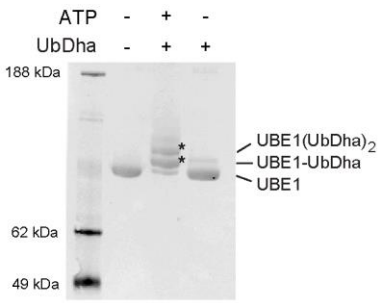

Supplementary Figure 3. Western Blot of UBE1 labeling reaction with UbDha (blotted against His-tagged UBE1) showing the UBE1-UbDha and UBE1(UbDha)$_2$ adducts (indicated by asterisks).

Nature Chemical Biology: doi:10.1038/nchembio.2084

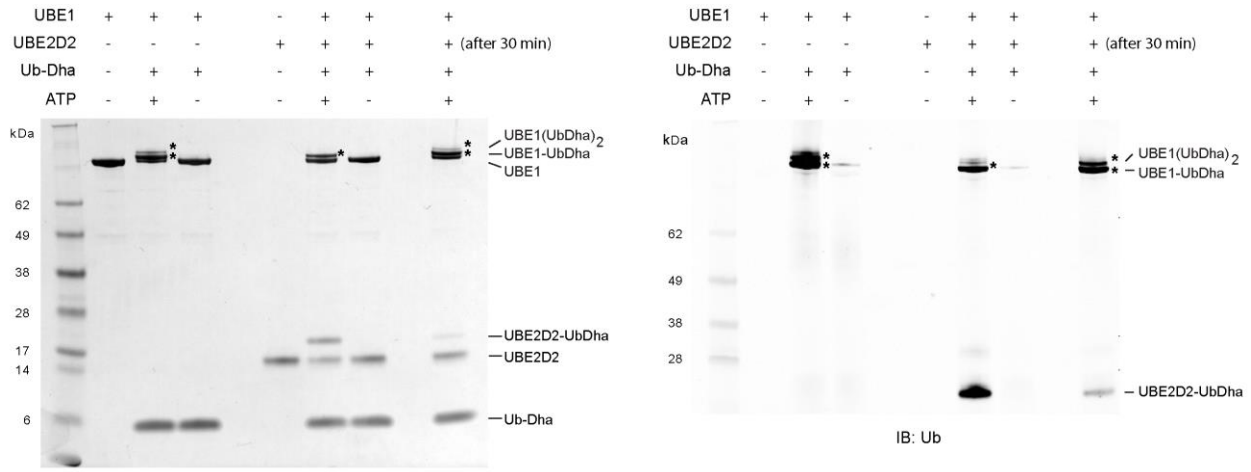

Supplementary Figure 4. Doubly loaded UBE1 intermediate is not formed in the presence of UBE2D2. Silver stain (left) and western blot against Ub (right). The asterisks indicate the thioether-linked UBE1-UbDha and UBE1(UbDha)$_2$ adducts.

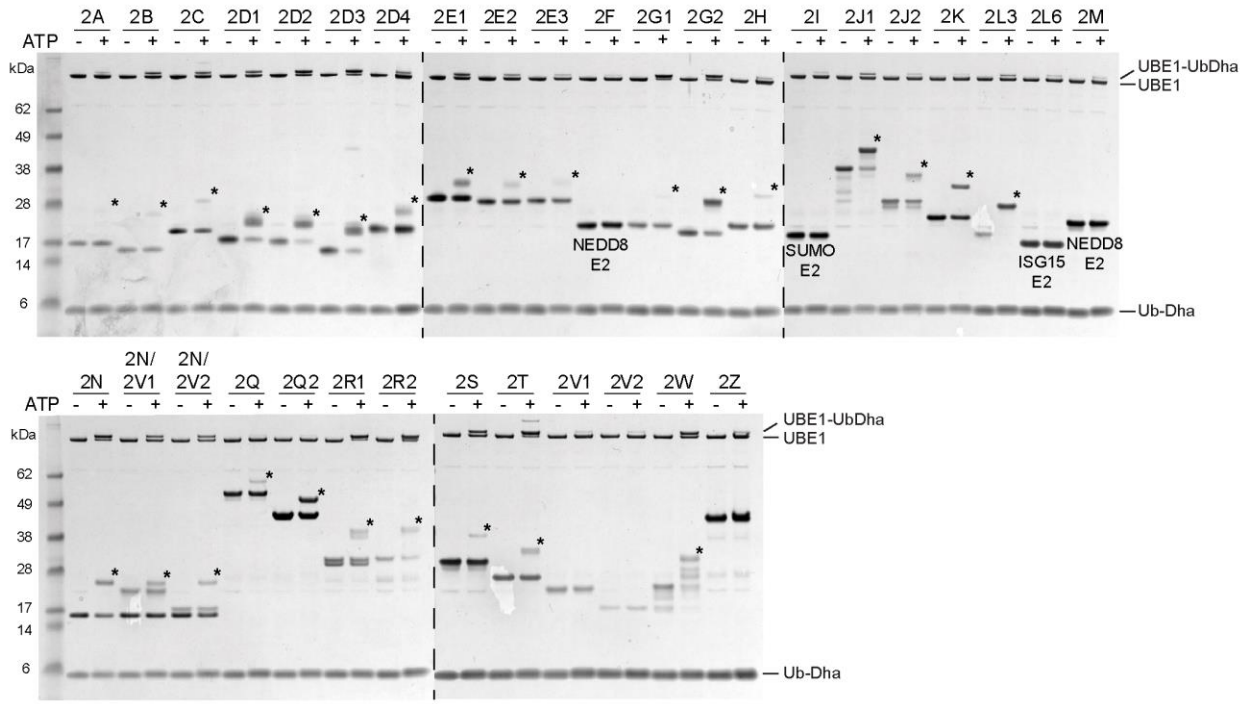

Supplementary Figure 5. UbDha labels 27 E2s specific for Ub transfer but not E2s employing Ubls. The asterisks indicate the thioether-linked E2-UbDha adducts. (E2-scan kit, Ubiquigent).Visualized by silver stain.

Nature Chemical Biology: doi:10.1038/nchembio.2084

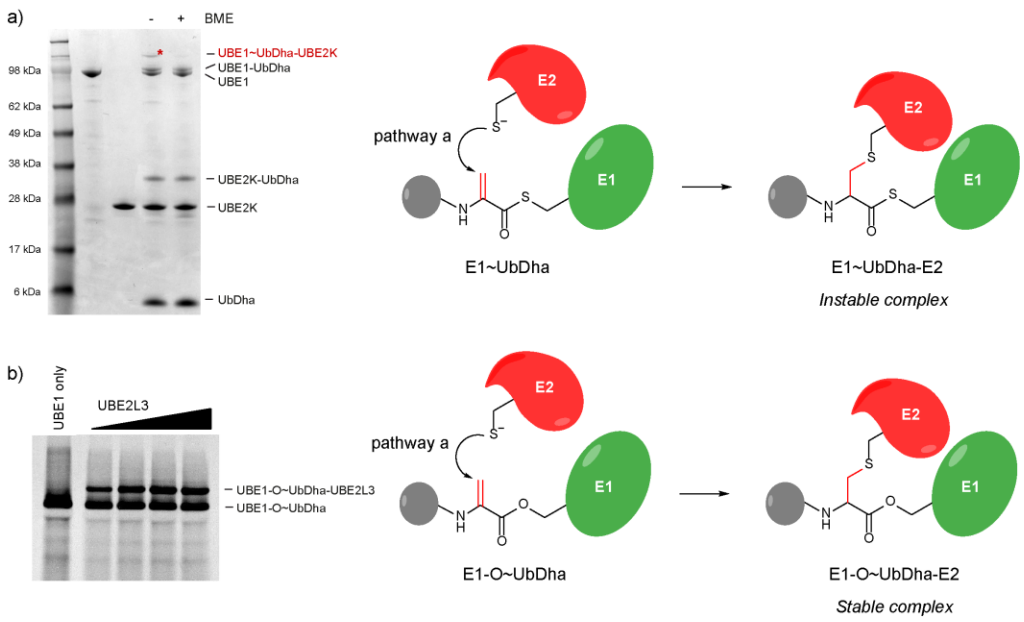

Supplementary Figure 6. A ternary complex is formed via a third pathway. The acceptor enzyme directly reacts with the Michael acceptor on the probe donating enzyme thioester adduct. a) SDS-PAGE analysis of UbDha reaction with UBE1 and UBE2K. Under non-reducing conditions the ternary complex is visible on gel, while under reducing conditions this instable complex is not (visualized by coomassie). b) In gel fluorescence analysis of Cy5-UbDha reaction with UBE1 active site Cys-Ser mutant and UBE2L3. Under reducing conditions the more stable ternary UBE1-O~UbDha-UBE2L3 is still visible.

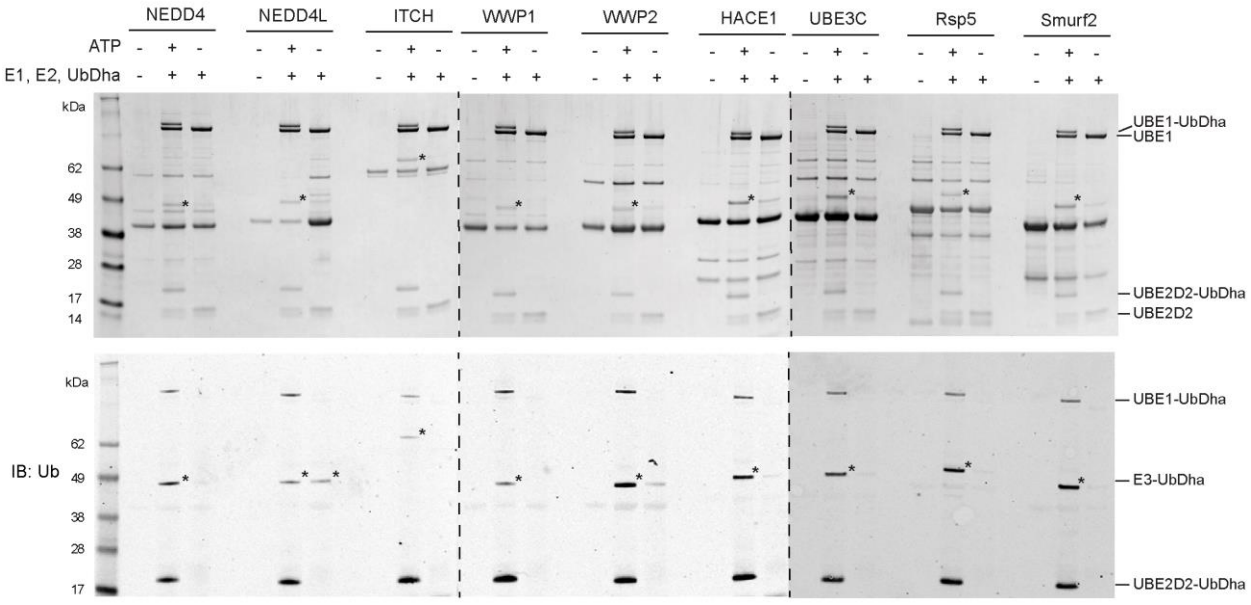

Supplementary Figure 7. UbDha shows reactivity towards E3 HECT enzymes under ATP dependent conditions. The asterisks indicate the E3-UbDha thioether-linked adduct. Visualized by silver staining (upper panel) and western blot against Ub (lower panel).

Nature Chemical Biology: doi:10.1038/nchembio.2084

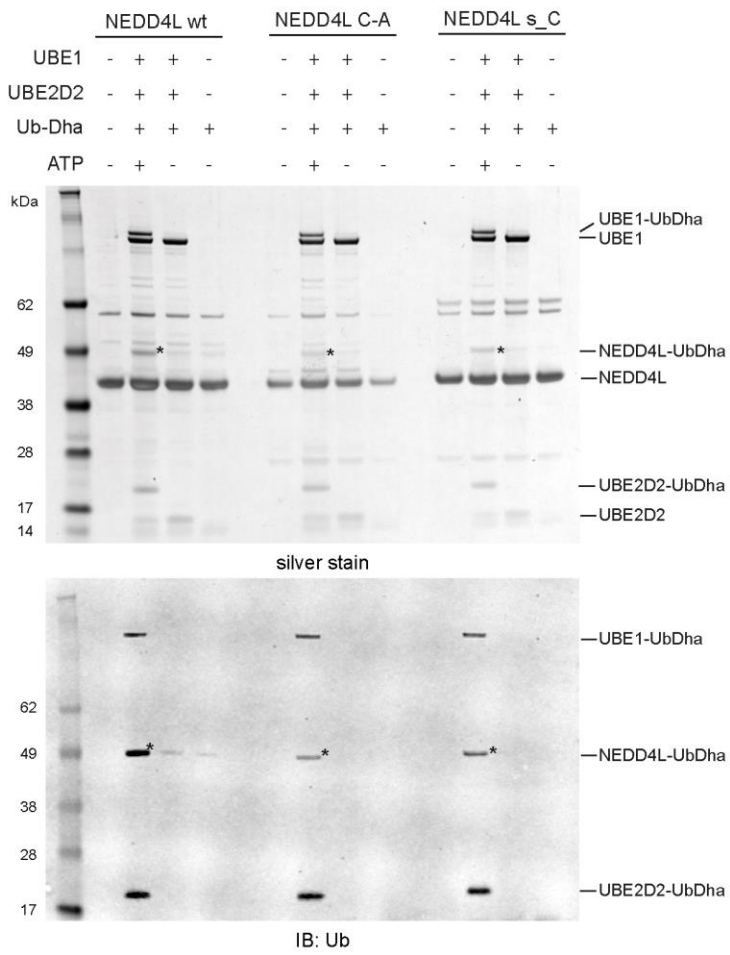

Supplementary Figure 8. Labeling of NEDD4L wt, Cys-to-Ala mutant and single Cys mutant with UbDha visualized by silver staining (upper panel) and western blot against Ub (lower panel). The asterisks indicate the thioether-linked NEDD4L-UbDha adduct.

Nature Chemical Biology: doi:10.1038/nchembio.2084

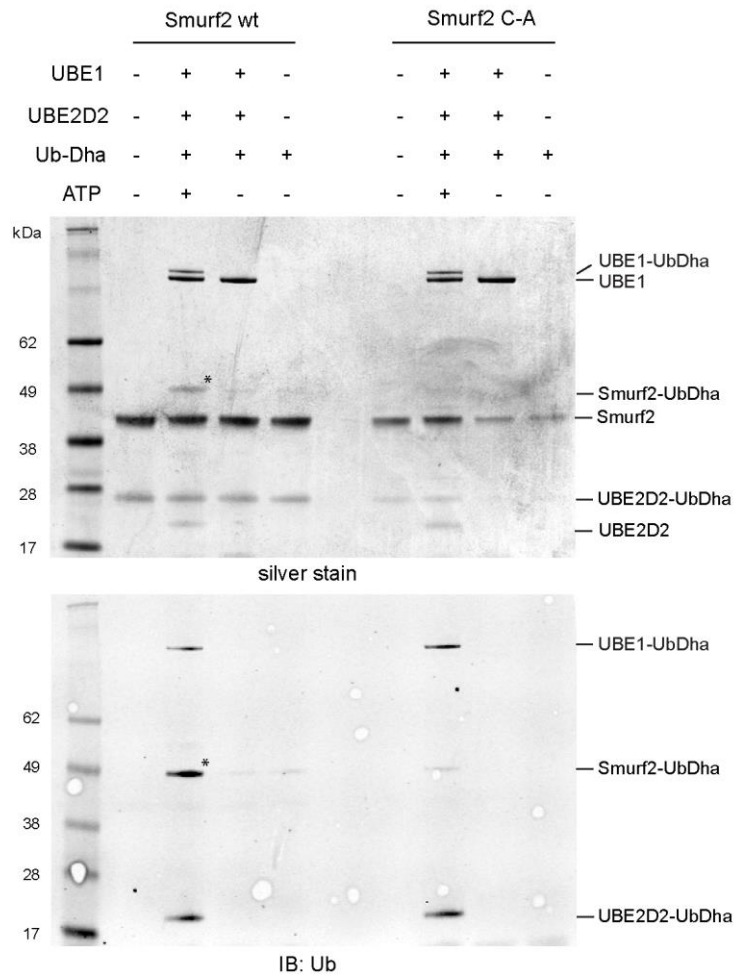

Supplementary Figure 9. Labeling of Smurf2 wt and Cys-to-Ala mutant with UbDha, visualized by silver staining (upper panel) and western blot against Ub (lower panel). The asterisks indicate the thioether-linked Smurf2-UbDha adduct.

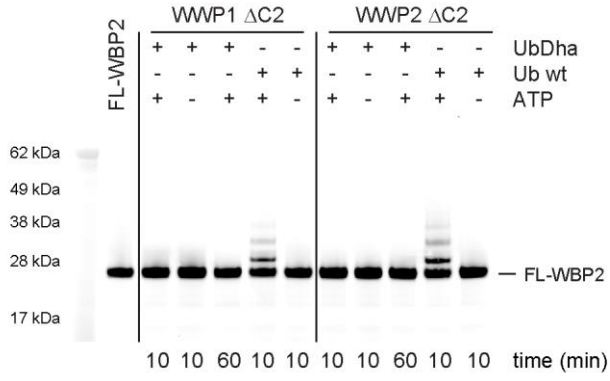

Supplementary Figure 10. Multiple turnover ubiquitination on substrate WBP2 does not occur with UbDha.

Nature Chemical Biology: doi:10.1038/nchembio.2084

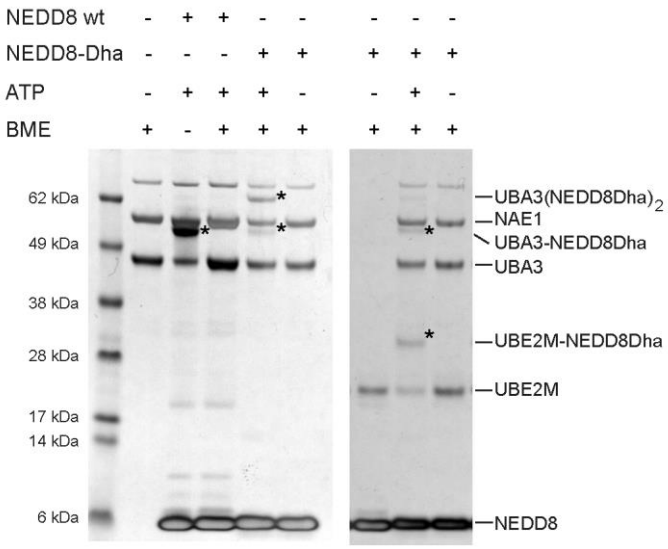

Supplementary Figure 11. NEDD8Dha shows covalent bond formation with the E1 UBA3 and E2 UBE2M (visualized by silver stain). Additionally a higher-running E1 band was detected, presumably corresponding to one NEDD8Dha marking the active site Cys and the other bound to the adenylation domain mimicking an E1 double-loaded intermediate (Supplementary Figure 12). The asterisks indicate the labeled enzyme adducts.

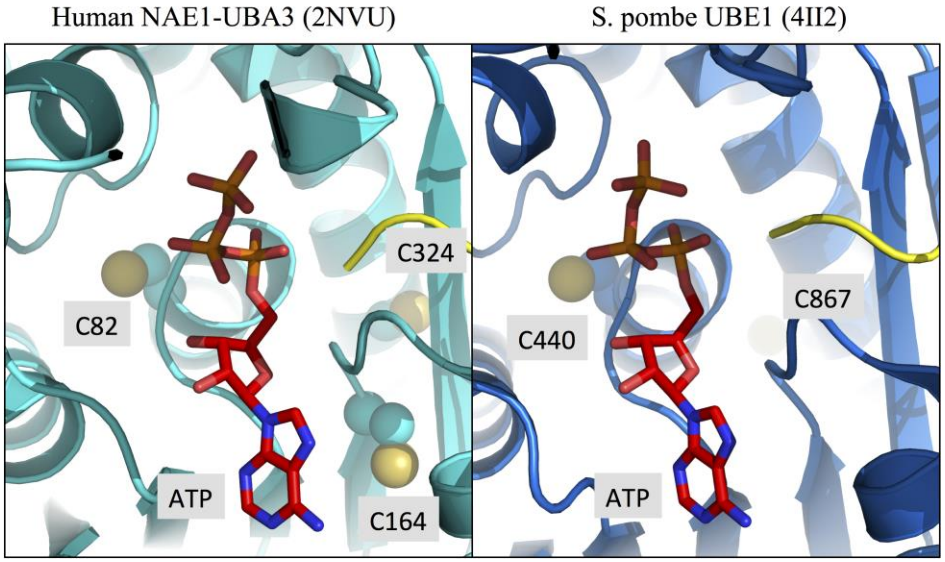

Supplementary Figure 12. Aligned E1 structures of the ATP binding site. The ATP binding site of NAE1 is flanked by three cysteines (Cys82, Cys164 and Cys324)[1], one of these (Cys82) is conserved in human UBE1 (Cys481). Note: There is no human E1 crystal structure available. Therefore we used a yeast UBE1 structure[2], as a homology model of human UBE1, to present the location of conserved cysteine near ATP (C481 of human UBE1 and C440 of Sp UBE1, human UBE1 and S. pombe share 53.8% sequence identity).

Nature Chemical Biology: doi:10.1038/nchembio.2084

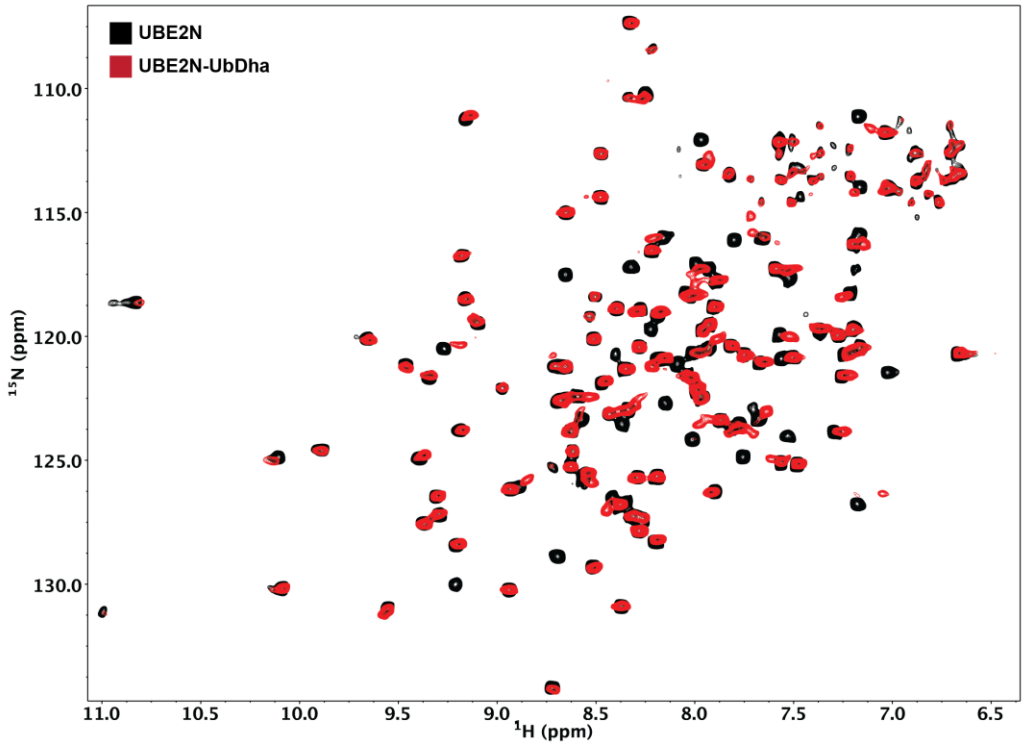

Supplementary Figure 13: Full ^{1}H, ^{15}N HSQC spectra of UBE2N (black) and thioether-linked UBE2N-UbDha (red).

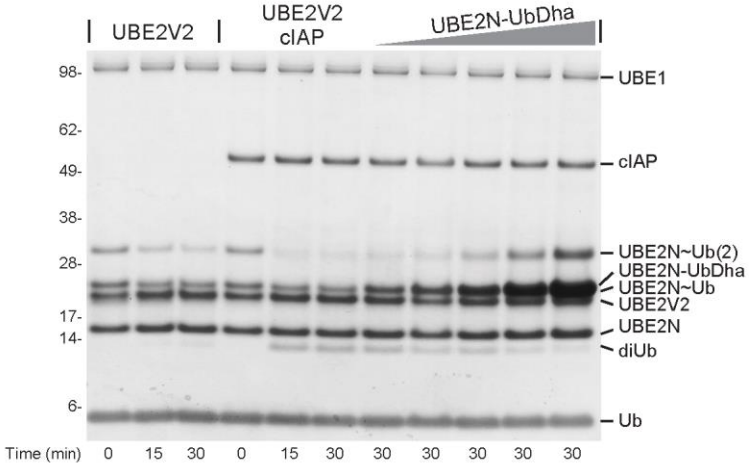

Supplementary Figure 14. Thioether-linked UBE2N-UbDha adduct can compete with downstream ubiquitination enzymes. Single-turnover ubiquitination assay monitoring the formation of diUb from thioester-linked UBE2N~Ub. Titration of the stable thioether-linked UBE2N-UbDha into the reaction results in diminished diUb production.

Nature Chemical Biology: doi:10.1038/nchembio.2084

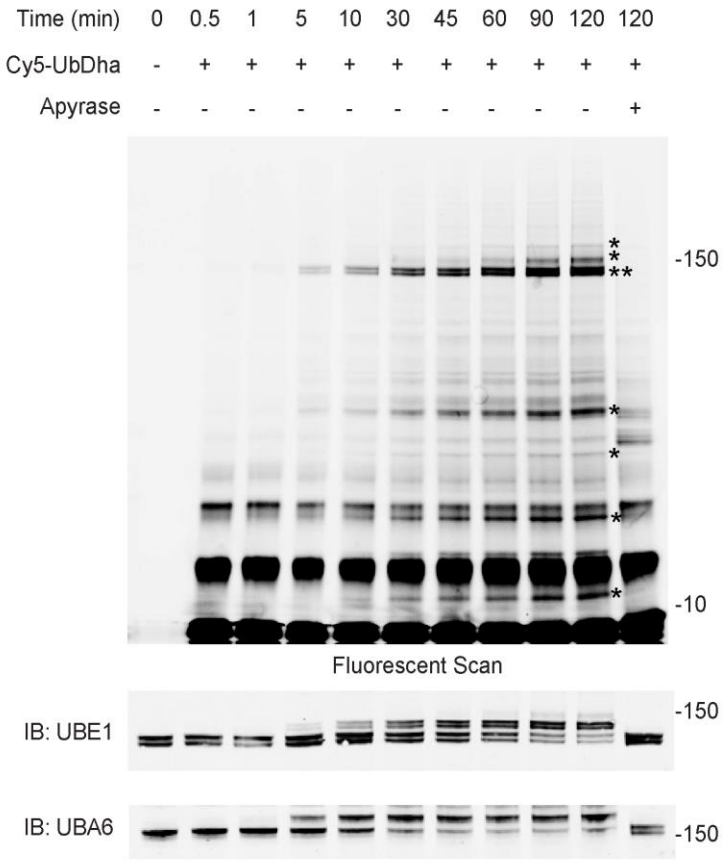

Supplementary Figure 15. Activation of UbDha in cell extracts. Time-course of HeLa cell lysates labeling with Cy5UbDha in the absence (-) or presence (+) of ATP scavenger apyrase. The asterisks indicate ATP-dependent bands.

Nature Chemical Biology: doi:10.1038/nchembio.2084

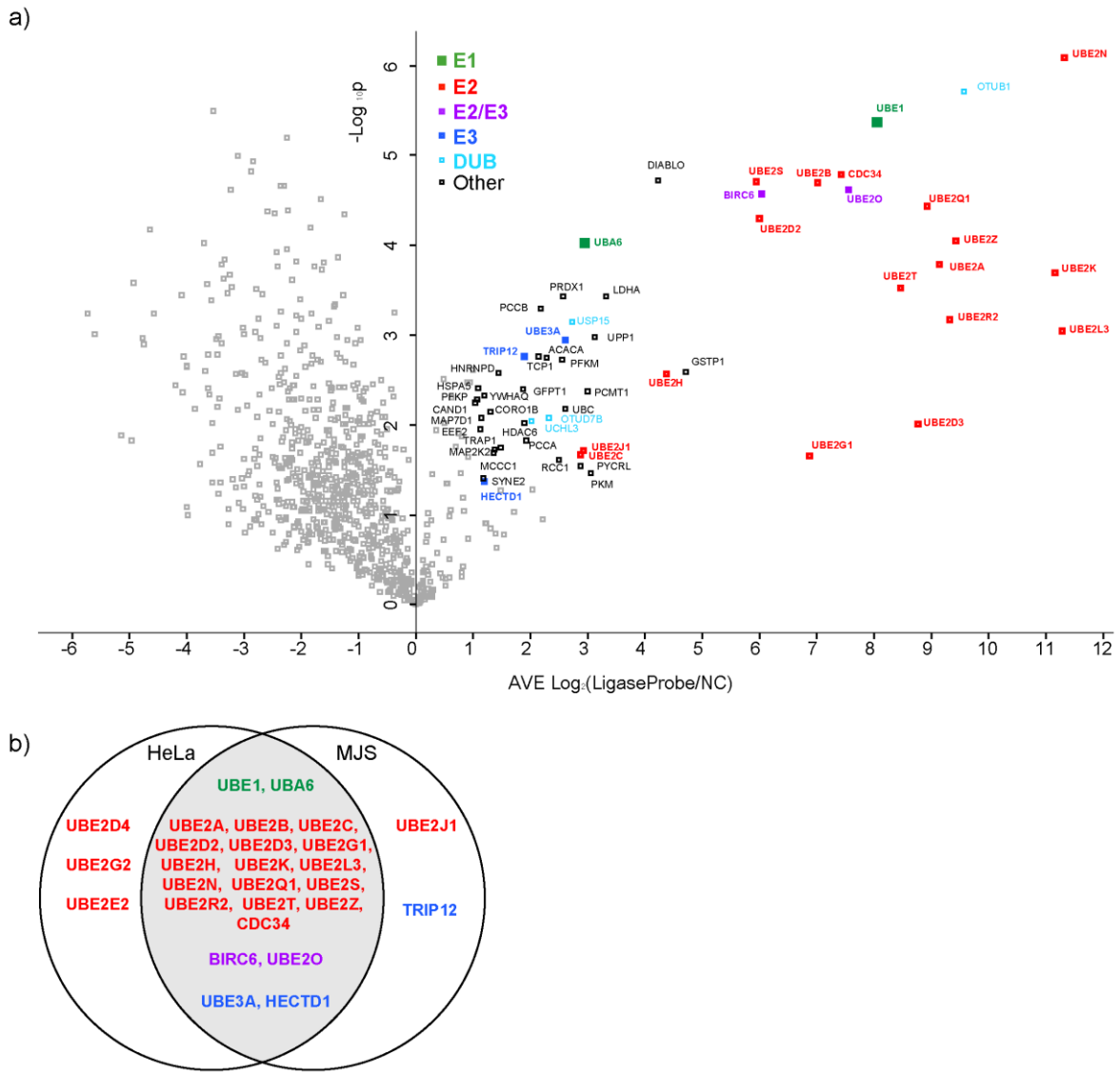

Supplementary Figure 16. Proteome-wide activity profiling of the Ub conjugation machinery in MelJuSo cells. **a**) Volcano plot of pairwise comparison of proteins bound to the Biotin-UbDha probe relative to the apyrase-treated negative control (negative $\log_{10}$ p-value, y-axis) as a function of average $\log_2$ fold enrichment (x-axis). Colored dots represent confidently identified ubiquitin machinery components as follows: E1 (green), E2 (red), HECT E3 (blue), hybrid E2/E3 (purple) and DUBs (light blue), with an average $\log_2$ ratio greater than 1 and with $p < 0.05$. Hits unrelated to the Ub cycle are marked in black, and proteins falling below the threshold are shown in gray. **b**) Venn diagram of shared Ub-conjugation enzymes recovered from HeLa and MelJuSo cells.

Nature Chemical Biology: doi:10.1038/nchembio.2084

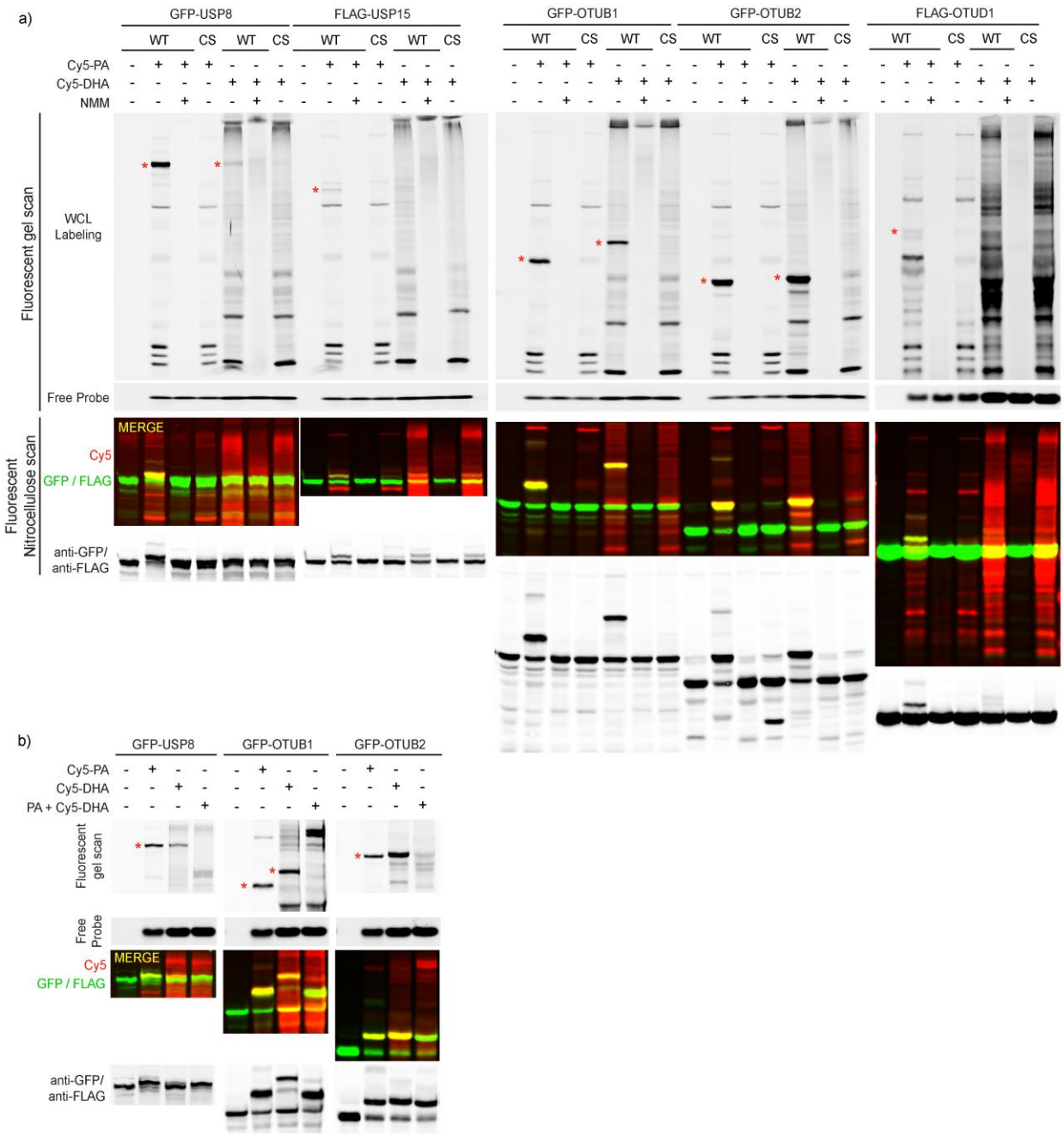

Supplementary Figure 17. DUB labeling: comparison of UbPA and UbDha. Labeling of DUBs in lysates of HEK293T cells transfected as indicated with Cy5-UbPA or Cy5-UbDha, visualized by fluorescence gel scan and immunoblotting against GFP or FLAG. **a**) Red asterisks indicate labeling of active DUBs. OTUB1 is doubly modified with UbDha, a known characteristic for OTUB1.[3] UbPA readily modifies all catalytically competent DUBs tested, while UbDha does not exhibit the same degree

Nature Chemical Biology: doi:10.1038/nchembio.2084

of reactivity. Mutations of active-site cysteine residues to serines abolished DUB labeling. **b**) Labeling of DUBs with Cy5-UbDha was completely abolished upon pretreatment with UbPA.

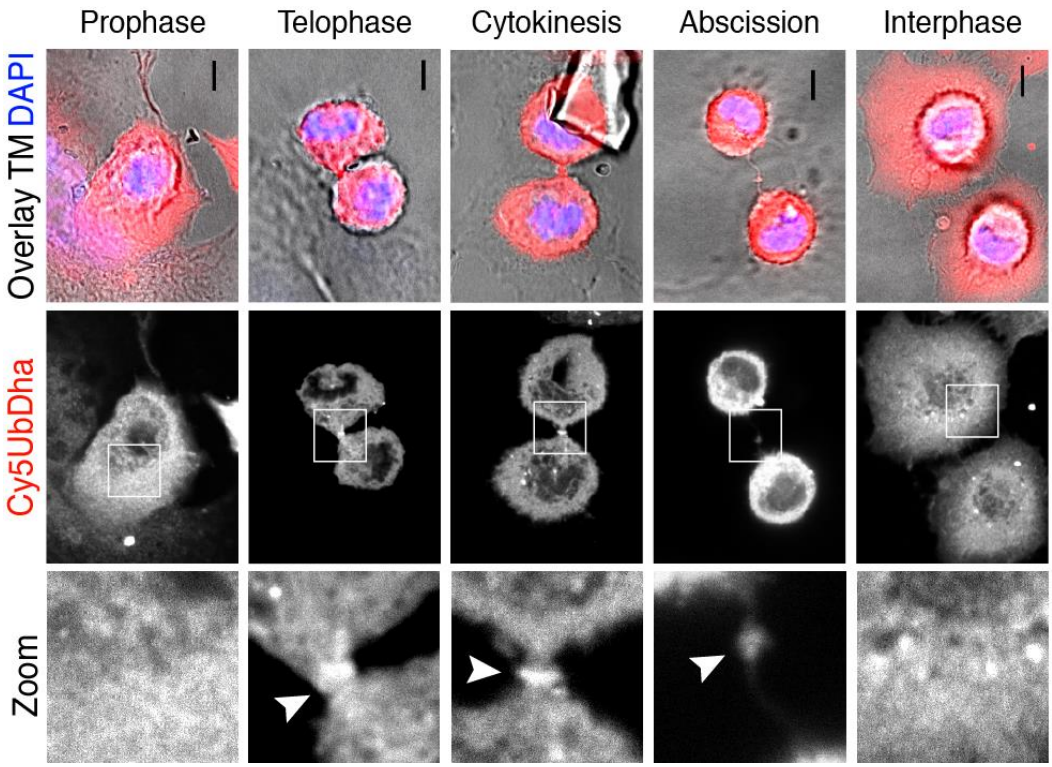

Supplementary Figure 18. Accumulation of Cy5-UbDha probe at the abscission site in diving cells. Cy5-UbDha probe (white, bottom panels) was introduced into HeLa cells by electroporation. Following 1 hr recovery period, cells were fixed and visualized by confocal microscopy. Representative images of cells harboring Cy5-UbDha undergoing various mitotic phases are shown; overlays correspond to Cy5 (red), nuclear DAPI (blue) and the transmission images; scale bars = 5 μm. Arrows point towards the site of abscission, where applicable.

Nature Chemical Biology: doi:10.1038/nchembio.2084

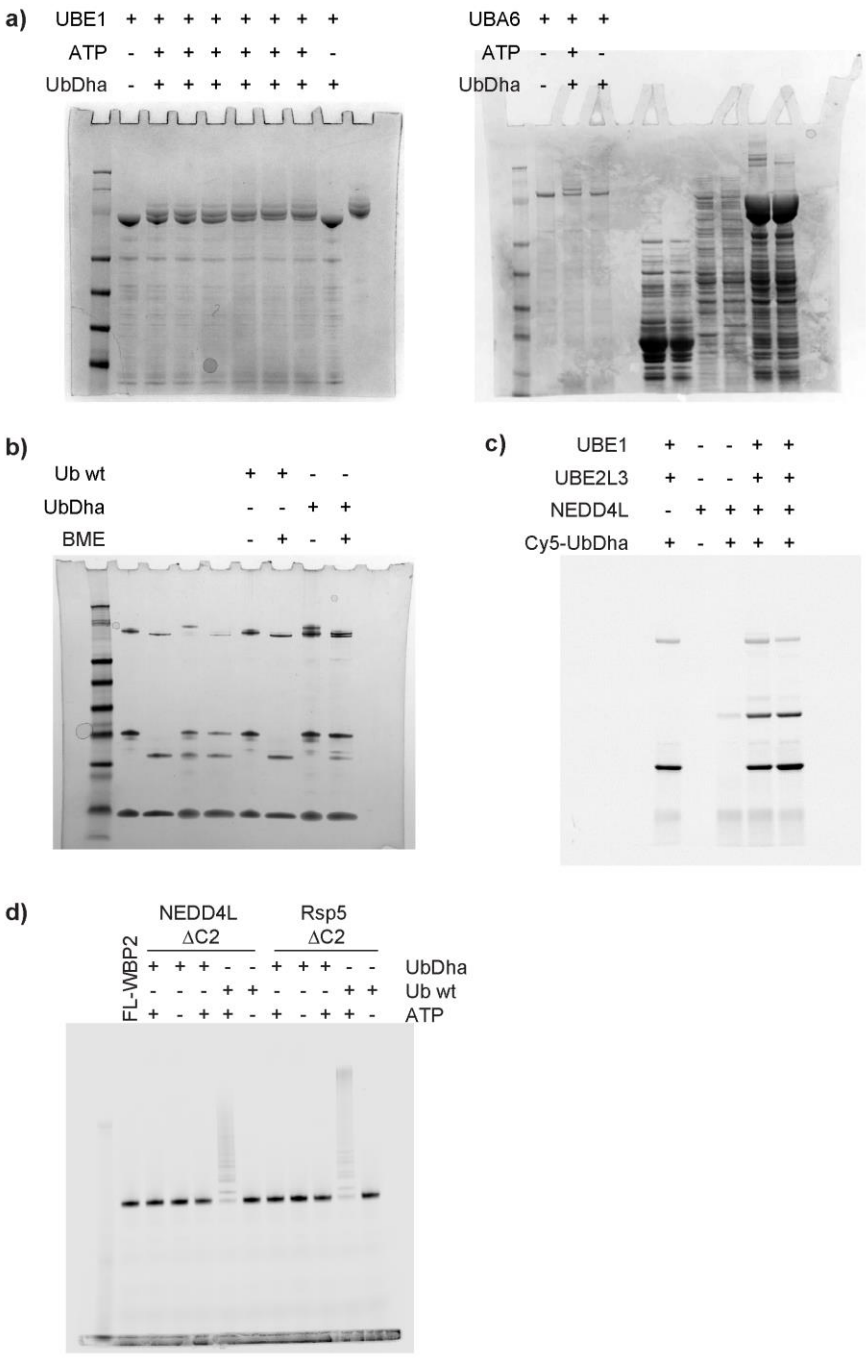

Supplementary Figure 19. Uncut gel images of Figure 2.

Nature Chemical Biology: doi:10.1038/nchembio.2084

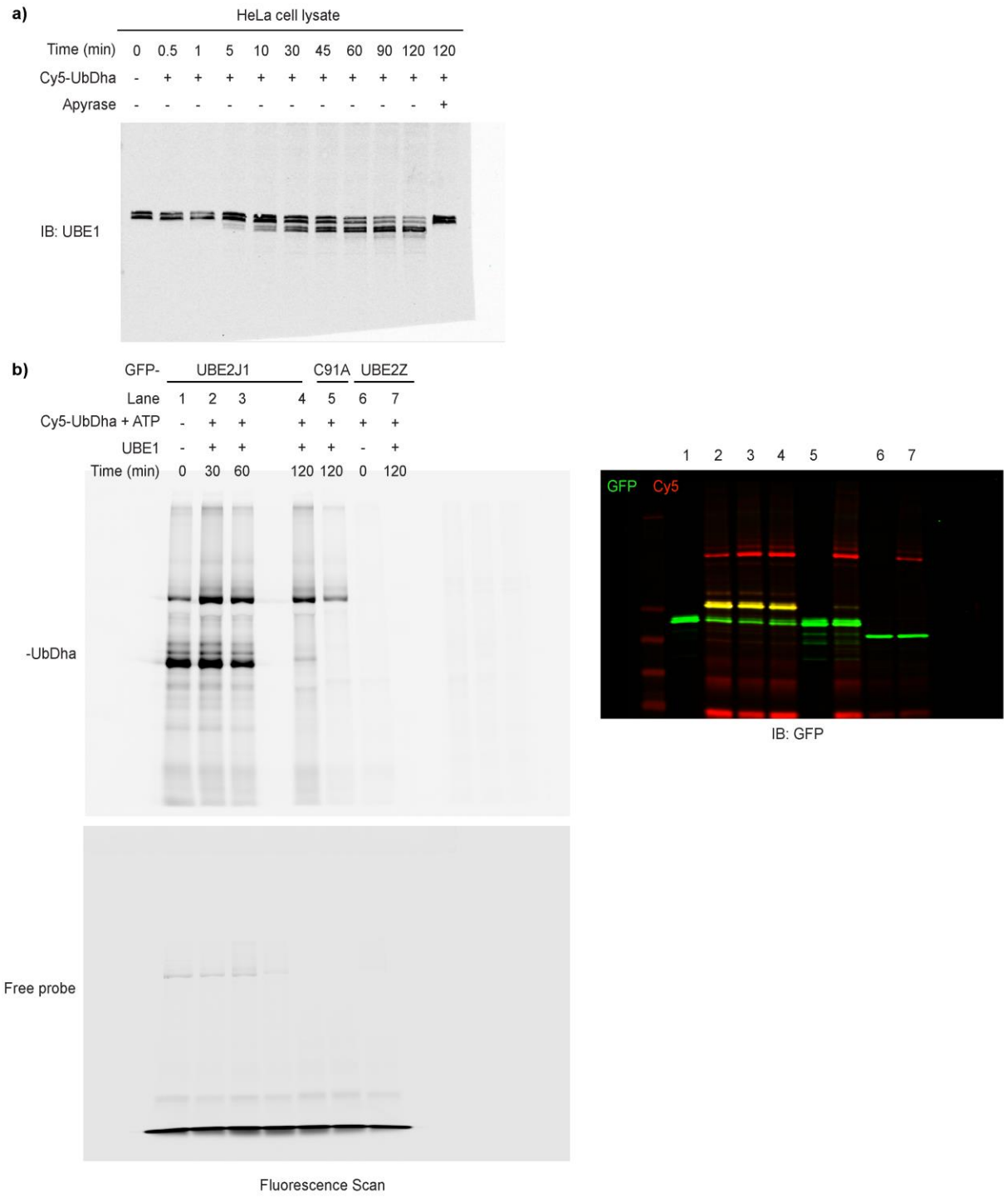

Supplementary Figure 20. Uncut gel images of Figure 4. **a**) Corresponds to Figure 4a, Full Fluorescence scan shown in Supplementary Figure 15; **b**) Corresponds to Figure 4c.

Nature Chemical Biology: doi:10.1038/nchembio.2084

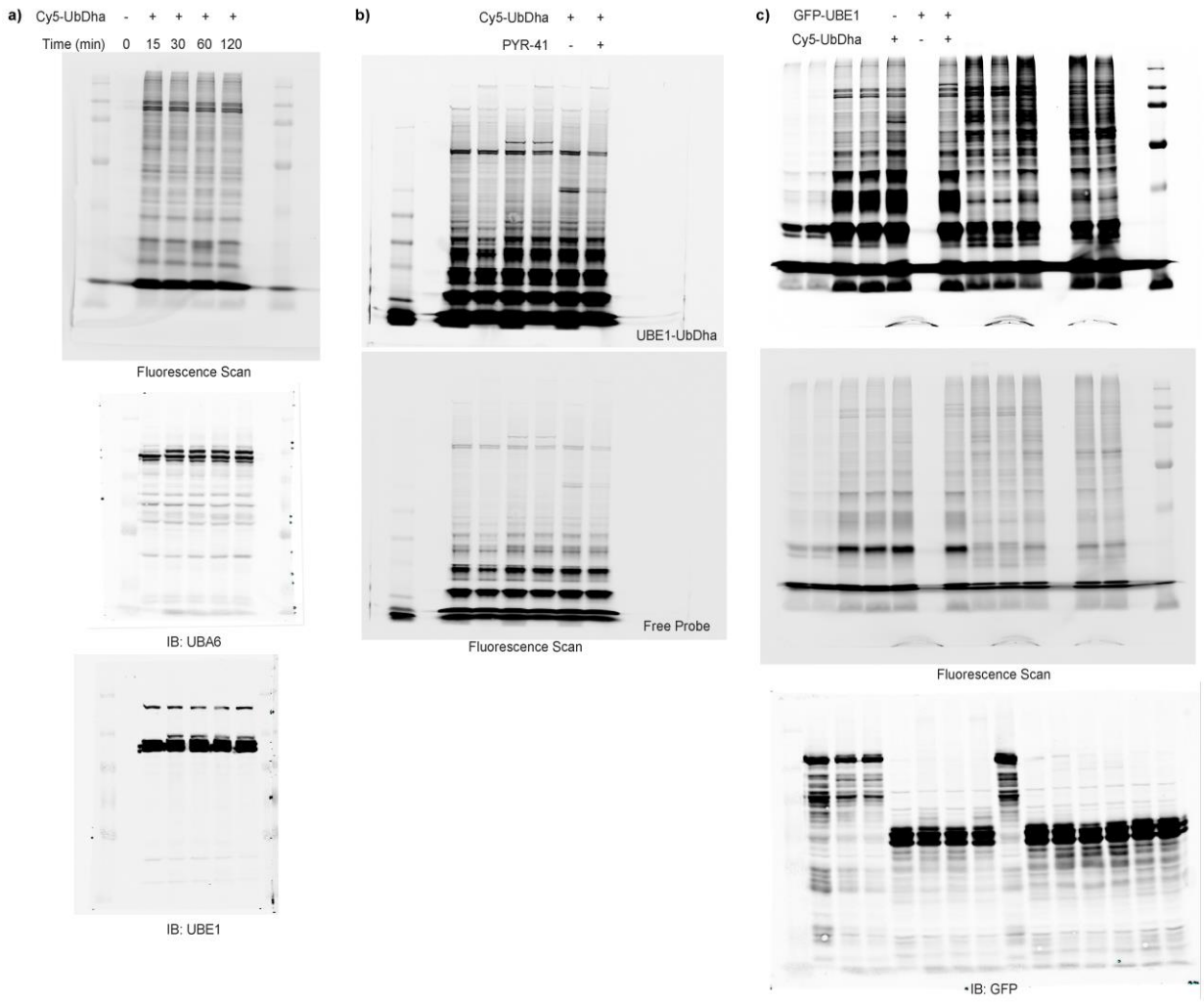

Supplementary Figure 21. Uncut gel images of Figure 5. **a**) Corresponds to Figure 5a; **b**) Corresponds to Figure 5b; **c**) Corresponds to Figure 5e.

Nature Chemical Biology: doi:10.1038/nchembio.2084

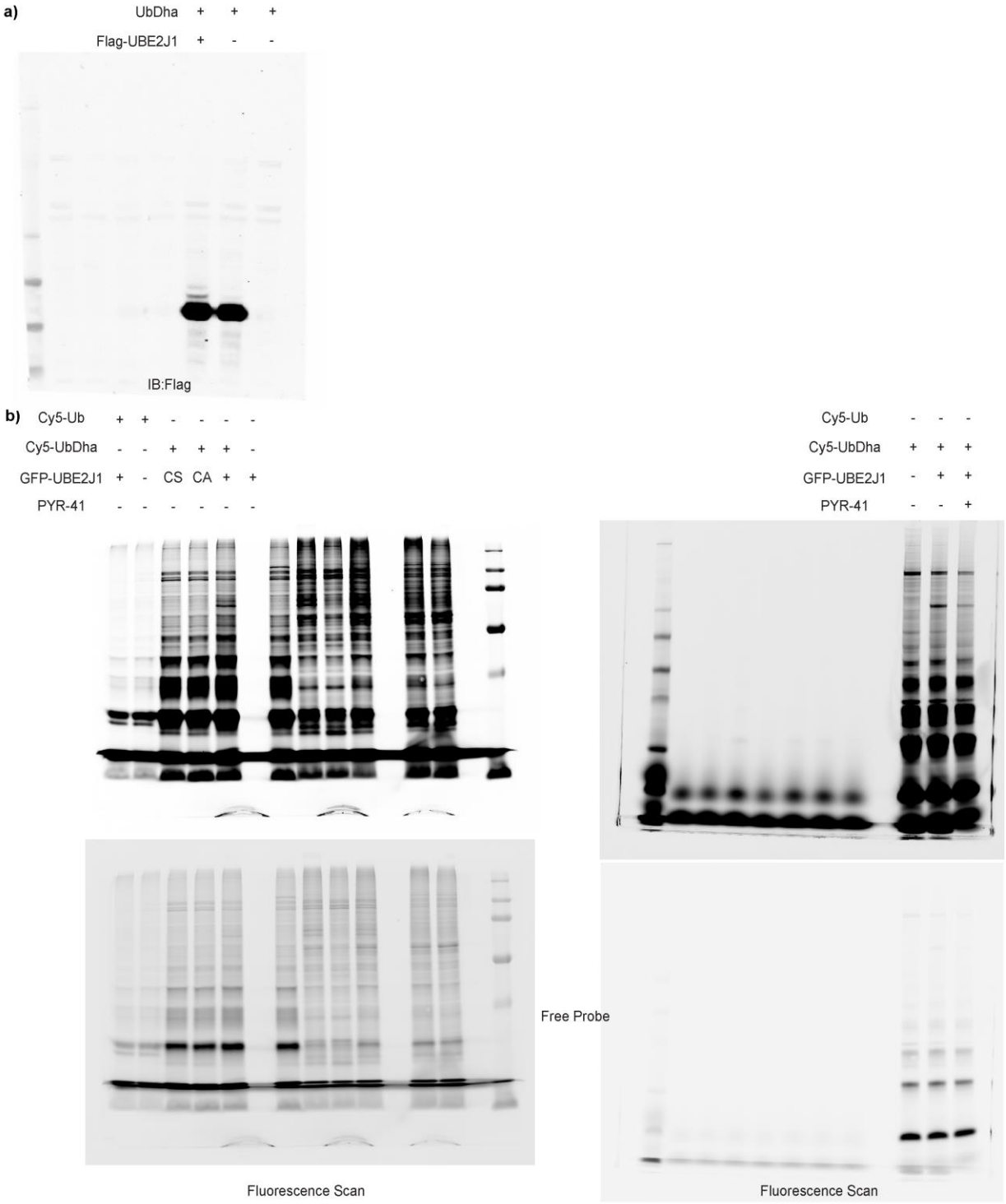

Supplementary Figure 22. Uncut gel images of Figure 6.

Nature Chemical Biology: doi:10.1038/nchembio.2084

Supplementary Table 1. Data collection and refinement statistics

	UBE2D3-UbDha
Data collection	
Space group	P 1 21 1
Cell dimensions	
a, *b*, *c* (Å)	42.13, 52.27, 53.62
α, β, γ (°)	90, 100.78, 90
Resolution (Å)	52.68 – 2.20 (2.28-2.20) *
R_{merge}	0.077 (0.76)
$I / \sigma I$	8.8 (2.0)
Completeness (%)	98.6 (99.6)
Redundancy	3.5 (3.6)
Refinement	
Resolution (Å)	52.68 – 2.20
No. reflections	40492
R_{work} / R_{free}	19.1 / 24.4
No. atoms	
Protein	1771
Ligand/ion	6
Water	77
B-factors	
Protein	49.4
Ligand/ion	67.9
Water	46.9
R.m.s. deviations	
Bond lengths (Å)	0.002
Bond angles (°)	0.58

*Highest-resolution shell is shown in parentheses.

References

1. Huang, D.T. *et al.* Basis for a ubiquitin-like protein thioester switch toggling E1-E2 affinity. *Nature.* **445**, 394-398 (2007).
2. Olsen, S.K. & Lima, C.D. Structure of a ubiquitin E1-E2 complex: insights to E1-E2 thioester transfer. *Mol Cell.* 49, 884-896 (2013).
3. Wang, T. *et al.* Evidence for bidentate substrate binding as the basis for the K48 linkage specificity of otubain 1. *J Mol Biol.* **386**, 1011-1023 (2009).

Nature Chemical Biology: doi:10.1038/nchembio.2084